Organic Conductors: From Charge Density Wave TTF−TCNQ to Superconducting (TMTSF)$_2$PF$_6$

Denis Jérome
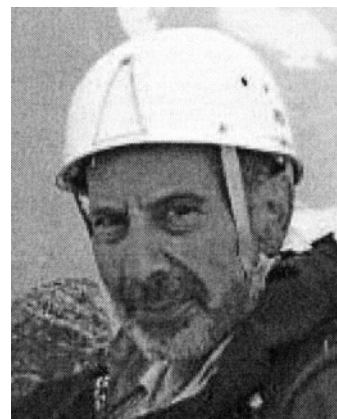
Laboratoire de Physique des Solides, UMR 8502, Université Paris-Sud, 91405 Orsay, France

Contents

D. Jérome graduated from the Université de Paris at CEA Saclay in 1965 with a Ph.D. on the Mott transition in doped silicon studied by electron−nucleus double resonance. After a postdoctoral position at the University of California, La Jolla, he started a research group on high pressure physics in metals and alloys at the Laboratoire de Physique des Solides, Orsay, in 1967. After numerous works related to low dimensional conductors, he discovered the organic superconductivity under pressure in the Bechgaard salt in 1979. He has had continuous activity in the same laboratory as Director of Research at CNRS in the field of low dimensional strongly correlated fermion systems. D. Jérome is a member of the Academy of Sciences. He enjoys mountain climbing as well.

1. Introduction

Superconductivity, that is, the possibility for electrons to flow through a conductor without any energy loss, has been the fuel for a very large number of industrial applications of physics in the twentieth century. Just to mention some of them which are i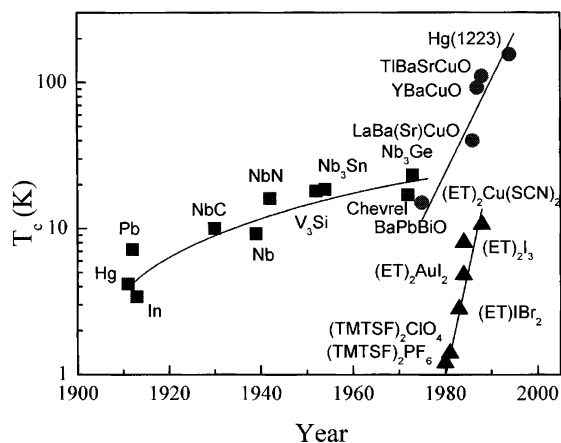mportant in current life, we have the power loss energy transfer, the production of very strong magnetic fields for medical imaging or for plasma confinement (the fusion problem) voltage standards, particle accelerators, and magnetic flux sensors.

This new state of matter was discovered somehow unexpectedly in 1911 in mercury with a critical temperature of $T_c = 4.15$ K by Onnes just after he had mastered the liquefaction of helium.[1] However, the phenomenon of superconductivity, in particular its T_c, is strongly dependent on the material in which it is to be observed. Therefore, over the years a lot of new metals and intermetallic compounds have been discovered with increased values of T_c, reaching a maximum which apparently leveled off at about 24 K in the 1950s; see Figure 1.

The absence of any satisfactory theory until 1957 did not prevent the applications of superconductivity which developed after World War II, but all these applications were bound to the use of liquid helium as the cooling agent, which is necessary to stabilize the superconducting state. It was only in 1986 that totally new types of copper oxides discovered by Bednorz and Müller led to drastically higher T_c.[2] This remarkable discovery was actually an outcome of the

Figure 1. Evolution of the superconducting critical temperature in metals and intermetallic compounds, cuprates, and organic conductors (one- and two-dimensional conductors).

quest for new materials able to show superconductivity under conditions as close as possible to ambient temperature. As to the possibility of superconductivity in materials other than metals, London in 1937[3] was the first to suggest that aromatic compounds under magnetic fields might exhibit a superconducting current running along aromatic ring systems (anthracene, naphthalene, ...) under a magnetic field,[3] although the concept of a synthetic metal had been previously launched by McCoy and Moore[4] when they proposed "to prepare composite metallic substances from non-metallic constituent elements". The first practical attempt to promote metal-like conduction between open shell molecular species came out in 1954 with the molecular salt of perylene oxidized with bromine,[5] although this salt was not very stable. In the 1960s, when superconductivity had already turned into practical applications, people were worrying about the existence of new superconductors which would no longer require the need for liquid helium, and Little made an interesting suggestion.[6,7] This was a new mechanism expected to lead to superconductivity at room temperature and to be observed in especially designed macromolecules. The idea of Little's mechanism is indeed strongly rooted in the isotope effect, which has been one of the great successes of the theory proposed in 1957 by Bardeen, Cooper, and Schrieffer[8] (BCS) for the interpretation of superconductors known up to that date. The attractive interaction between electrons (or holes) which is a prerequisite for the Bose condensation of electron pairs into the superconducting state for the BCS theory relies on the mass M of the ions which undergo a small displacement when the electrons are passing close to them, namely, $T_c \propto M^{-1/2}$. In the excitonic mechanism of Little it is an electronically polarizable entity which is used instead of the usual polarizable ionic lattice. Consequently, the small electronic mass m_e would lead to an increased T_c of the order of $(M/m_e)^{1/2}$ times what is observed in a conventional superconductor. This was the beginning of the concept of room temperature superconductivity, still a dream for scientists in the twenty-first century.[9] As far as materials are concerned, the model of Little was based on the use of a long

conjugated polymer such as polyacetylene together with the grafting of polarizable side groups.[10] This formidable task in synthetic chemistry did not succeed, but the idea to link organic metallicity and one-dimensionality happened to be stimulating for the development of organic superconductors, although a lot of basic physical problems had been overlooked in the seminal paper of Little.[6]

This article is a survey of some physical properties of organic compounds which have played an important role in the discovery of organic superconductivity. The presentation of this review follows an historical unfolding, since the research project on conducting organic solids triggered by Little's idea[6] aimed at stabilizing superconductivty at high temperature. Although the discovery of organic superconductivity took sixteen years of intense activity in the physics and chemistry communities, the early efforts led to the synthesis of facinating new compounds. These are the one-dimensional (1D) charge-transfer conducting compounds undergoing a Peierls instability at low temperature which prevents the stabilization of superconductivity (even under pressure), whose study has been very important for the future of the domain. Organic superconductors came six years later, in 1979.

We have emphasized, in particular, TTF–TCNQ, on which a lot of precursor work has been accomplished, and also the $(TM)_2X$ series of organic salts where organic superconductivity has been discovered and further studies on the electron localization due to correlations (Mott localization) have been carried on. One-dimensionality of the electron energy spectrum is the common feature to all these conductors, as shown by anisotropic optical and transport properties. In addition, their metallic phase is characterized by the unsuitability of the classical Drude model to explain the very peculiar behavior of the frequency dependent conduction. For TTF–TCNQ, a narrow collective mode due to long-lived charge density fluctutations is emerging at zero frequency out of an elecron–phonon induced pseudogap in the far-infrared regime. Such a narrow zero frequency mode is also observed in the pseudogap of the conducting state of $(TM)_2X$ at low temperature, although for these latter compounds the pseudogap can be attributed to the remnants of the Mott localization due to Umklapp scattering of the electrons of a quarter-filled conductor. The superconducting phase of one-dimensional organic conductors will be only briefly discussed in this review, as the experimental situation is not yet consensual. It is certainly unconventional with sign changes of the gap as required by the unusually large sensitivity of the superconducting state to nonmagnetic defects, but an unambiguous choice discriminating between p and d types should await more experimental studies.

2. Early Suggestions

2.1. First Organic Conductors

All organic conductors belonging to the first generation are given by linear arrays of organic molecules forming either radical ion salts or charge-
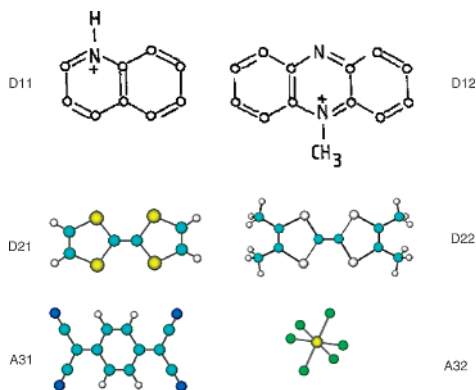
Figure 2. Some molecular components entering the synthesis of organic conductors, quinolinium and *N*-methylquinolinium (D11 and D12), TTF and TMTTF (D21 and D22), the acceptor TCNQ (A31), and the monoanion PF_6 (A32).

transfer complexes. Diverse kinds of counterions not carrying any magnetic moment have been used: inorganic, organic, or metal complexes. These counterions acting as oxidizing or reducing agents guarantee charge compensation, but they do not affect directly the physical properties of the solid. Such is the case as long as they possess a spherical symmetry. When their symmetry is no longer spherical (see for instance the case of ReO_4 in section 3.4), anion ordering at low temperature can double the length of the unit cell along the stacking axis and in turn trigger a metal−insulator transition.

Typical examples for such sytems are given by π electron molecules[11] able to accept or donate their electron depending on their electroaffinity *A* or on their ionization potential *I*. Tetracyanoquinodimethane (TCNQ) is the historical example of an acceptor molecule ($A = 2.88$ eV) which can be easily reduced to form the open shell anion radical $TCNQ^{\bullet-}$ when it is placed in contact with electron donors (Figure 2). The single unpaired electron occupies the lowest unoccupied π level (LUMO) of the molecule and is located mainly on the terminal dicyano methylene carbon groups.

Examples are given by one to one salts $K^+TCNQ^{\bullet-}$, where K denotes a monocation, or one to two complexes $K^+(TCNQ^{\bullet-})_2$. $Qn^+(TCNQ^{\bullet-})_2$ (Qn = quinolinium) is a complex salt in which TCNQ molecules stack face to face, building up columns with an intermolecular spacing within each column shorter than the usual van der Waals distance.[12,13] The conductivity of this salt amounts to $\sigma = 70$ (Ω cm)$^{-1}$ at 300 K, rising slightly below room temperature up to a maximum of $\sigma = 74$ (Ω cm)$^{-1}$ at 240 K, and is activated at low temperature. In addition, with the Seebeck coefficient being constant and large over a broad temperature range, the insulating character of $Qn^+(TCNQ^{\bullet-})_2$ cannot be ascribed to usual semiconducting properties of band semiconductors, although from the viewpoint of band theory the unpaired electron on the TCNQ stacks is collective and, together with the uniform stacking, metallic conduction could be anticipated. It was pointed out by Shchegolev[12] that this salt could be located on the insulating side of a Mott transition. Other salts such as $Et_2NH^+(TCNQ^{\bullet-})_2$ exhibit a strongly dimerized
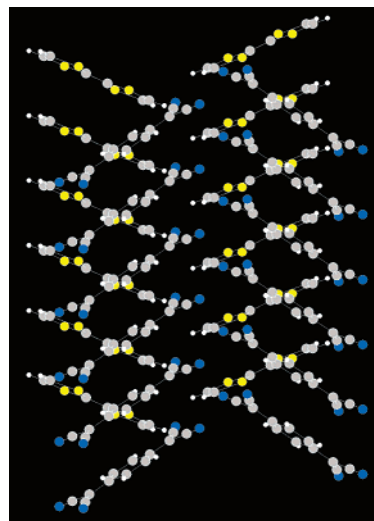

Figure 3. Side view along the *a*-axis of the molecular stacking of TTF−TCNQ along the *b*-axis.

structure. The transport properties are activated, and the susceptibility obeys the singlet/triplet excitation of the alternated Heisenberg antiferromagnet. Another system with uniform packing of the molecules is provided by the segregated stacks in the radical ion salt $NMP^+(TCNQ)^{\bullet-}$, in which the diamagnetic closed shell NMP^+ ions give one electron to be shared with the acceptor TCNQ molecules.[14] For a long time, this system has been considered as a radical ion salt with conduction provided by the TCNQ stacks only. However, X-ray studies in solid solutions of NMP^+- and phenazine molecules (which are neutral and closed shell) have shown that the electronic conduction is carried by both donor and acceptor stacks.[15,16] Furthermore, even in the case of pure NMP−TCNQ there exists some back charge transfer from TCNQ to NMP^+ molecules of about $^1/_3$ electron per NMP^+ molecule, leading in turn to partially charged LUMO bands of both molecules with an inverted curvature in reciprocal space similar to what is observed in the next system TTF−TCNQ.

2.2. TTF−TCNQ

TTF−TCNQ is the prototype of the charge-transfer compounds where HOMO and LUMO bands of the open shell donors and acceptors, respectively, contribute to the conduction.[17] It has also been the first organic conductor to present a large conductivity in a wide temperature domain down to 59 K, where a sharp metal to insulator transition is observed.[18] TTF−TCNQ is a material comprising uniform segregated and parallel stacks with π orbitals contributing to two conduction bands in a tight binding picture (Figure 3). The overlap of the molecular orbitals being largest along the stack direction and much weaker between them makes the electron dispersion one-dimensional. To a first approximation, the energy depends only on the electron wave vector along the $b*$ direction in the reciprocal space.

The lowest electron energy on the TCNQ stacks occurs when all molecular orbitals are in-phase (at $k = 0$ in reciprocal space). On the other hand, the band structure of the TTF stacks is inverted with an
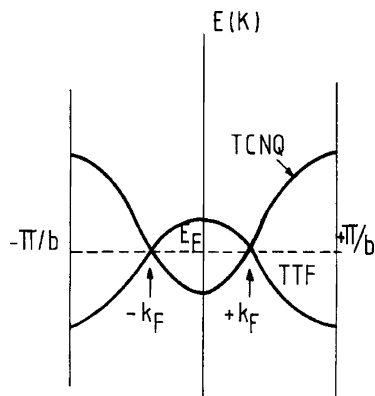
Figure 4. Inverted band structure of TTF−TCNQ.

energy maximum at the zone center (Figure 4). Such a band crossing picture ensures that both bands intersect at a single Fermi wave vector $\pm k_F$ in order to preserve the overall neutrality.[19] Consequently, all states between $-\pi/b$ and $+\pi/b$ are occupied with the restriction that between k_F and $+k_F$ occupied states belong to the TCNQ band while outside this domain they pertain to the TTF band.[20] The mere fact that the charges can delocalize in TTF−TCNQ shows that the on-site Hubbard repulsion U does not overcome the band energy $4t_{\parallel}$ gained in the band formation. However, Coulomb repulsions do play an important role, especially for the magnetic and structural properties of the TTF stacks (vide infra).

The announcement by Heeger together with the Pennsylvannia group[21] in 1973 of a giant conductivity peak of the order of 5×10^4 or 10^5 (Ω cm)$^{-1}$ at 60 K just above the very sharp transition toward the insulating state at lower temperature triggered a tremendous interest in this compound and in organic conduction altogether. The authors of this discovery even suggested that this enormous value of the conductivity (about the copper conductivity at room temperature with a hundred times less carriers per unit cell) could be ascribed to precursor signs of an incipient superconductor. It was claimed that the softening of the phonon mode at the wave vector $2k_F$ could enhance the superconducting binding energy and in turn lead to superconducting fluctuations in the 1D domain above a long range superconducting order masked by the onset of a metal−insulator transition. This was the traditional thinking at that time, since it was believed from the study of the A15 superconductors that soft phonon modes were responsible for the high values of their T_c.[22] This early work suggested that the metal−insulator transition could be the manifestation of the instability due to a spontaneous distortion of the lattice with a wave vector $2k_F$, as had been predicted by Peierls in 1955 for a one-dimensional conductor.[23] While the enormous conductivity peak announced in 1973[21] did not survive the extensive experimental investigations performed by other groups, it has certainly boosted the research effort in the field of one-dimensional conductors and organic conductors, which led to the discovery of organic superconductivity in 1979.
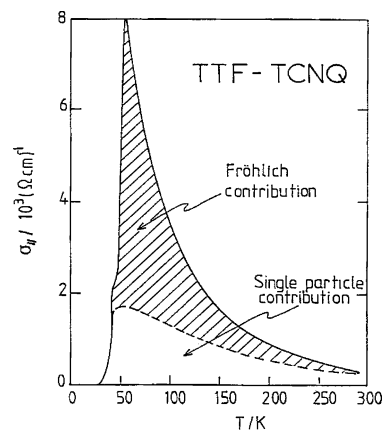
Figure 5. Temperature dependence of the TTF−TCNQ conductivity showing the fluctuating CDW contribution to the total conduction. (Reprinted with permission from ref 25. Copyright 1982 Taylor and Francis (http://www.tand-f.co.uk/journals).)
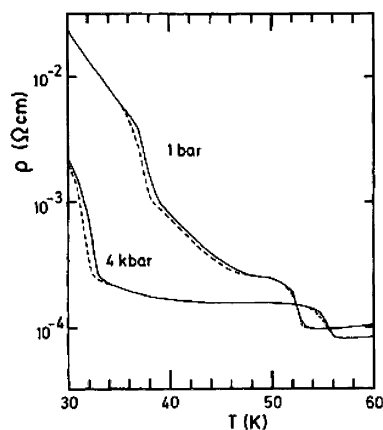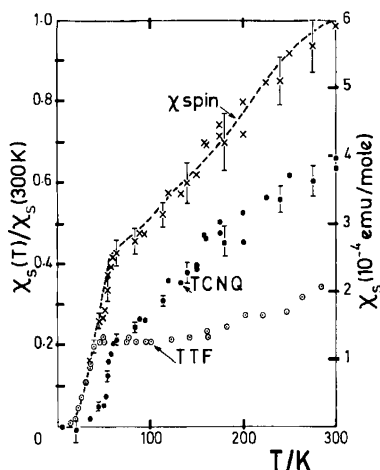

Figure 6. Temperature dependence of the TTF−TCNQ resistivity at 1 bar and under 4 kbar displaying transitions at T_H, T_M, and T_L with the hysteretic region between T_M and T_L. (Reprinted with permission from ref 26. Copyright 1978 American Physical Society.)

2.3. TTF−TCNQ: Structural and Electronic Transitions

The value for the room temperature conductivity of TTF−TCNQ is rather consensual;[18,21,24] namely, $\sigma_{\parallel}$ = 400 ± 100 (Ω cm)$^{-1}$. However, the giant increase of conductivity up to ≈10^6 (Ω cm)$^{-1}$ at 60 K claimed by the Pennsylvania group in some single crystals has never been reproduced by any group. Instead, a normalized increase of about 20 has been frequently reproduced in several laboratories (Figure 5).

We shall see in the following that, although modest, such an increase of conductivity is already the signature of collective effects of this 1D conductor. As can been seen from the behavior of the resistivity with a change in temperature, from 54 K and down a cascade of phase transitions destroys the metallic character progressively (Figure 6). Such a behavior has been fairly well explained from diffraction, transport, magnetic, calorimetric, and imaging data by the onset of a charge density wave state in a system of conducting chains of TCNQ and TTF coupled by a Coulombic interaction.[25]

Two major transitions can be seen in transport: one at T_H = 54 K, where the conductivity drops by a

Figure 7. Temperature dependence of the TTF−TCNQ susceptibility decomposed into TCNQ and TTF contributions from Knight shift and EPR data. (Reprinted with permission from ref 27. Copyright 1984 Institute of Physics.)
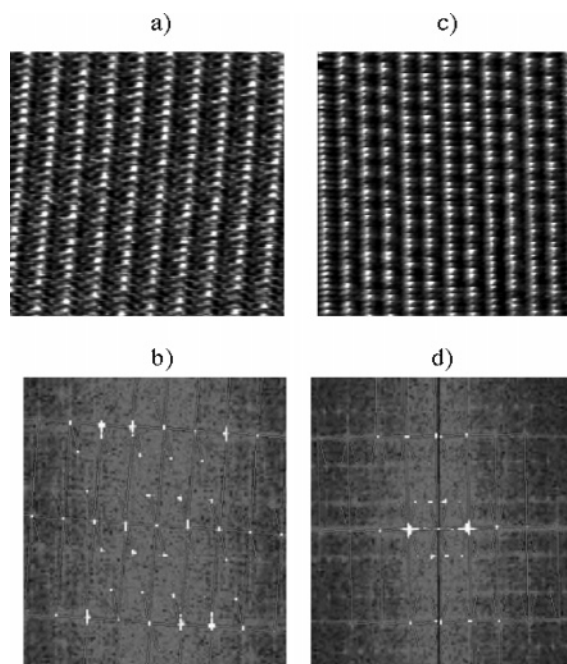

Figure 8. Scanning tunneling microscope view of TTF−TCNQ taken at 63 K (top) and at 49.5 K (bottom) with the 2D Fourier transform. (Reprinted with permission from ref 33. Copyright 2003 American Physical Society.)

Figure 9. Scanning tunneling microscope view of TTF−TCNQ and Fourier transforms taken at 39 K (a and b) and 36 K (c and d). (Reprinted with permission from ref 33. Copyright 2003 American Physical Society.)

factor of 2, and another at $T_L = 38$ K,[28] which is the signature of a sharp first-order transition toward an insulating ground state. Furthemore, between T_M and T_L the transport data reveal an hysteretic behavior.[26] Besides transport, susceptibility studies performed via the measurement of the ^{13}C Knight shift in selectively enriched samples[27] have shown (Figure 7) that the spin gap in the TTF stack becomes fully open at T_L while the loss of the spin degrees of freedom of the TCNQ stacks is already complete below T_H with no marked spin gap on the TTF stack between T_H and T_L (although a noticeable dependence of the conductivity is observed in the same temperature domain.[29]

The experimental confirmation of a Peierls transition came from the results of X-ray diffuse scattering experiments and elastic neutron scattering, which have contributed a great deal to the study of the phase transitions in TTF−TCNQ.[30−32] To summarize, between T_H and T_M there is $2a \times 3.4b \times c$ superstructure. Between T_M and T_L the period in the a direction evolves continuously and jumps discontinuously to $4a$ at T_L. Such experiments have provided the clear-cut signature for a Peierls instability of a 1D conductor. They have also given the first accurate determination of the charge transferred between TTF and TCNQ molecules. With a periodicity along the stack axis, $3.4b$, the charge transfer amounts to $\rho = \frac{2}{3} \times 4 = 0.59$ at low temperature.

Useful results related to the charge density wave transitions of TTF−TCNQ have been obtained recently using a scanning tunneling microscope working in an ultrahigh vacuum at low temperature.[33] A picture of the ab plane taken at 63 K is displayed in Figure 8 where the 1D structure of parallel chains is clearly visible. Those containing a triplet of balls are the TCNQ molecules, while the doublet has been assigned to TTF molecules. The distances between chains or between units within each chain in Figure 8 compare fairly well with the $a = 1.23$ nm and $b = 0.38$ nm lattice constants of TTF−TCNQ. Below 54 K a two-dimensional superstructure becomes apparent on the TCNQ chains. Its period can be measured
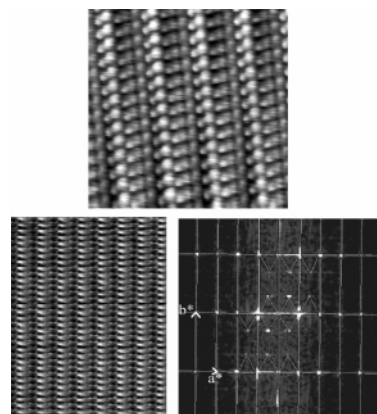
with much accuracy by performing a 2D Fourier transform of the real space pattern and gives $2a \times 3.39b$ in the ab plane. On further cooling below T_M, the transverse modulation becomes incommensurate without noticeable change along b (Figure 9). Below T_M the CDWs are active on both kinds of stacks and the 2D superlattice can be described by plane waves with the wave vectors either $q_+ = [+q_a(T), 2k_F]$ or $q_- = [-q_a(T), 2k_F]$ leading to energetically equivalent configurations.[34,35] The wave vector q_+ gives rise to a charge modulation such as $\rho(r) = \rho_+ \cos(q_+r + \theta_+)$, which is a CDW of fixed amplitude and a phase varying like q_aa along the a direction, and similarly for the q_- wave vector. Consequently, the diffraction pattern of the CDW state should display domains characterized by the vectors q_+ and q_-. There also exists another possibility, namely: the superposition of the two plane waves q_+ and q_-, which leads to a CDW with constant phase but a modulated ampli-
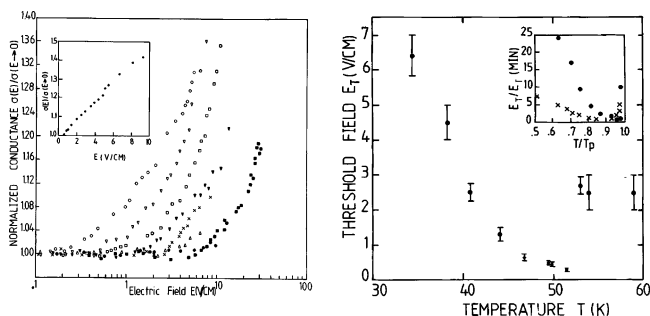
Figure 10. TTF−TCNQ: nonlinear conduction in the CDW phase (left) and temperature dependence of the threshold field (right). (Reprinted with permission from ref 44. Copyright 1987 American Physical Society.)

tude along the a direction:[36,34] a double-q configuration. The only solution which can take advantage of the commensurability energy related to the transverse commensurate periodicity $4a$ through the fourth order Umklapp term in a Landau-Ginzburg expansion is the double-q configuration.[34] This means that both wave vectors are simultaneously activated below 38 K with four satellite spots at $\pm q_+$ and $\pm q_-$ in the reciprocal space around a main Bragg spot. On the other hand, it has been pointed out that the phase modulated solution should be the most stable one in the incommensurate transverse wave vector temperature regime and also the only one to provide a smooth onset at 49 K.[34] The presence of a microscopic coexistence of vectors q_+ and q_- below 38 K has been shown by X-ray diffuse scattering[37] and a structural determination.[38] Such results can be confirmed by the Fourier transform of the real space image of the ab plane taken below T_L (Figure 9), showing that the two wave vectors q_+ and q_- are simultaneously activated in the same region of the real space. However, in the temperature domain between T_M and T_L, where the transverse wave vector is incommensurate, X-ray experiments cannot tell the difference between an amplitude modulated configuration and one in which the phase is modulated with an equal number of domains with q_+ and q_-. Figure 9 obtained at 39 K shows that STM being a local imaging technique can solve this problem. The Fourier transformed image shows that the modulation is described by a single wave vector which can be either q_+ or q_- in large domains. This is the phase modulated solution for the problem of frustrated CDWs on two chains which was expected to give the lowest energy when the transverse ordering is incommensurate.[34]

2.4. Charge Density Wave Sliding

A consequence of the CDW formation in TTF−TCNQ is the possibility to observe a collective conduction channel with a conductivity becoming nonlinear when the applied electric field exceeds a certain threshold field (Figure 10).[39−41] The existence of nonlinear conduction was well-known from quasi 1D inorganic materials such as $NbSe_3$ or $K_{0.3}MoO_3$ below the Peierls transition, where the nonlinear conduction has been interpreted as resulting from CDW depinning.[42] When the electric field overcomes the threshold field, the CDW sliding contributes to a

collective current which adds to the regular single particle and ohmic current.[43] Nonlinear conduction has been observed below T_H in TTF−TCNQ with E_T reaching a minimum of 0.25 V/cm at 51.2 K in the narrow temperature interval in which TTF−TCNQ is a single chain CDW.[44] A fast increase of E_T is observed on cooling below T_M when a CDW arises on the TTF chains, with E_T becoming of the order of $1-10$ V/cm. This rise of E_T has been understood in terms of the sliding of joint CDWs on TTF and TCNQ stacks moving together in the same direction with a pinning mechanism governed by impurities. According to a Landau type theory of the CDW formation, the enhancement of the impurity pinning mechanism is linked to the growth of a CDW on TTF chains and the existence of a Coulomb attraction between oppositively charged chains.[45] In the absence of any coupling between TTF and TCNQ chains, an electric field would lead to CDW motion in opposite directions on the two-chain systems because of the electron (TCNQ) and hole (TTF) character of the electronic bands.

More information regarding the nature of the mechanism responsible for the pinning of the CDWs has been provided by irradiation induced defects revealing a linear increase of the threshold field with the concentration of defects.[44] This result provides evidence for an adjustment of the flexible CDW around the pinning center; this is the strong pinning situation considered by Lee and Rice.[46] Other features such as the existence of an ac response to a dc bias exceeding the threshold field have also been observed in TTF−TCNQ.[47]

2.5. The High Temperature Phase: Precursor Conductive Effects

The interest in 1D conductors lies also in their providing a new channel of electronic conduction which involves a coherent sliding of all electrons building up a fluctuating incommensurate CDW in every chain[39] above the Peierls transition. It is a collective process inasmuch as it can give rise to conductivity even in the presence of an energy gap in the single particle energy spectrum. In the 3D ordered state CDWs lose their 1D character as they become coupled to their neighbors via the interchain electrostatic interactions. Consequently, the entire CDW assembly is efficiently pinned by infinitesimal amounts of impurities. The 3D CDW condensate can still contribute to a channel of conductivity, provided it is depinned by a large enough electric field, as shown by the study of TTF−TCNQ at $T < T_H$. Above the phase transition, the situation is quite different, since, with a transverse coherence length smaller than the interchain distance, 1D CDWs of large intrachain coherence length can exist in a wide temperature domain, as has been demonstrated by the data of X-ray diffuse scattering experiments in the high temperature regime.[30,48] Hence, it is conceivable that such long-lived fluctuations could contribute to a free sliding conduction during their lifetime.[40,41] In the proposal of Bardeen and co-workers, the rigid

translation of CDWs thermally excited gives a contribution to the conductivity such as

$$\sigma_F(\omega) \propto \langle|\Delta|^2\rangle \frac{\gamma}{\gamma^2 + \omega^2} \qquad (1)$$

where γ^{-1} is the lifetime of the CDW fluctuations due to the decay into electron−hole pairs and $\langle|\Delta|^2\rangle$ is the average of the fluctuating amplitude of the order parameter of the CDWs in the 1D regime.[25] It has been shown in ref 25 that amplitude fluctuations can still remain large well below the mean field 1D transition if the normalized Ginzburg critical regime is larger than unity. Since $\langle|\Delta|^2\rangle$ is proportional to the intensity of the diffuse scattering around $2k_F$, fluctuating sliding conduction can be anticipated in TTF−TCNQ. Various mechanisms can suppress the fluctuation conductivity via pinning:

1. If the coherence length becomes comparable to the mean distance between impurities.

2. If interchain correlations between CDWs of opposite charge become important (i.e. in the very narrow 3D fluctuation regime in the vicinity of T_H) and suppress the motion of the fluctuations in opposite directions.

3. If a low order of commensurability between the CDW wavelength and the lattice is achieved.

We shall see below that none of the above-mentioned pinning mechanisms are active in the high temperature regime under ambient pressure.

Despite the well established 1D CDW fluctuations in TTF−TCNQ,[48] the interpretation of the metallic conduction of this 1D conductor, namely, single particle versus collective mechanisms, has been the subject of intense discussions in the past.[49]

Although very brittle, organic samples such as TTF−TCNQ and all subsequently discovered materials, $(TM)_2X$ and so forth, have been studied rather easily under hydrostatic pressure using various pressure techniques (helium gas pressure up to 15 kbar, Teflon cell clamp up to about 35 kbar, and Bridgman anvils above that), it is now widely appreciated that high pressure measurements at low temperature have played a decisive role in the study of most molecular conductors and in the ultimate discovery of organic superconductivity.

2.6. TTF−TCNQ under High Pressure

Making the conductor less one-dimensional via the increase of the overlap between stacks (applying an hydrostatic for example) was considered as one possible remedy to suppress the one-dimensional Peierls instability[50,28] and enable the superconducting instability (which should be less sensitive to the 1D character) to develop at high temperature. So, this has been the motivation for the beginning of the study of TTF−TCNQ under pressure.[28,51] The phase diagram of TTF−TCNQ obtained from transport measurements is displayed in Figure 11 and shows that the transition at T_H exhibits a slow evolution toward higher temperatures under pressure. In addition, above 15 kbar a clear peaking of the transition is observed in a narrow pressure domain of about 4 kbar width. In this pressure domain, the transition
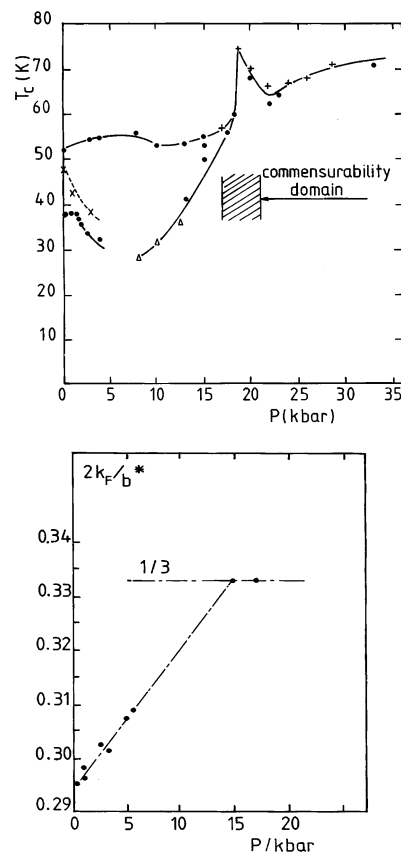
Figure 11. Temperature−pressure phase diagram of TTF−TCNQ showing the commensurability domain around 14−19 kbar (top) (Reprinted with permission from ref 25. Copyright 1982 Taylor and Francis (http://www.tandf-.co.uk/journals)).) and direct measurement of the Fermi wave vector from neutron scattering experiments under pressure (bottom). (Reprinted with permission from ref 52. Copyright 1981 Elsevier.)

becomes first order, as shown by the one degree hysteresis observed at the transition.[26] This phase diagram can be understood in terms of a commensurability between the CDW and the underlying lattice, as expected from a Landau theory of the transition introducing a third-order term in the development of the free energy in terms of the order parameter.[53] As shown in Figure 4, it is the particular shape of the inverted band structure of TTF−TCNQ broadening under pressure and the requirement that neutrality must be preserved which give the possibility for the Fermi wave vector to increase under pressure with a concomitant increase of the charge transfer, from $\rho = 0.55$ carrier/unit cell at 1 bar up to $\rho = 0.66$ or 2/3 and $\lambda_{CDW} = 3b$ in the pressure window 15−20 kbar. This assumption has been confirmed by a direct measurement of the Fermi vector in neutron scattering experiments under pressure.[52] The commensurability occurring under pressure is a direct consequence of the pressure induced band broadening which has been calculated for TCNQ, TSeF, and TTF bands versus the b-axis parameter.[54] This band broadening is in fair agreement with the experimental data of the pressure dependence of the plasma edge,[55] which in the tight binding model reads $\omega_p^2 \propto t_\parallel$, leading to an increase of ω_p of about 1% kbar^{-1}. All pressure coefficients related to the bare bandwidth (commensurability,
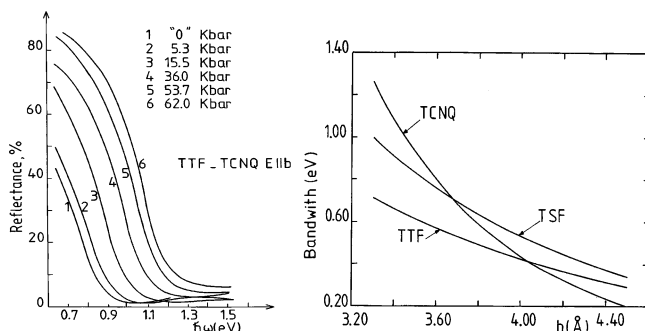
Figure 12. TTF−TCNQ: reflectance under pressure (left) (Reprinted with permission from ref 55. Copyright 1978 American Physical Society.) and bandwidth pressure dependence (theory) according to ref 54 (right). (Reprinted with permission from ref 54. Copyright 1977 The Royal Swedish Academy of Sciences.)

plasma edge) are of this latter order of magnitude while the strong pressure coefficient of the dc conductivity suggests that transport is governed by a scattering time which is very sensitive to pressure ($\approx$28% kbar^{-1}). What has been learnt for the behavior of TTF−TCNQ under pressure is that the stabilization of superconductivity under pressure in TTF−TCNQ is hopeless, at least below 35 kbar. This is due to the nature of the transverse coupling needed to stabilize long range ordering: an electrostatic coupling instead of the interchain hopping, as will become the case for the low temperature magnetic phases in the (TM)$_2$X series. It is also clear that a noninteracting electron picture is inappropriate for the description of the electron scattering time while it remains in fairly good agreement with the data of optical reflectance under pressure (Figure 12). Similarly, huge pressure dependences of transport and susceptibility are observed in organic superconductors (see section 3), but experimental data regarding the shift of the plasma edge under pressure are still lacking in these materials.

2.7. Fluctuating Conduction

This section intends to present how the conditions under which fluctuating conduction can be suppressed can be met under pressure. This possibility is based on the third-order commensurability between the CDW and the underlying lattice which is achieved when TTF−TCNQ is driven through the pressure domain around 19 kbar. From a theoretical point of view, two contributions can contribute to the conductivity of the metallic phase in the 1D regime:[56] first, an increase in the fluctuation conductivity which is proportional to the mean amplitude of the fluctuations and, second, an increase in the single particle *resistivity* due to the onset of a Peierls pseudogap which is also proportional to the amplitude of the fluctuations. The pressure dependence of the longitudinal conductivity of TTF−TCNQ in the metallic domain reveals a drop of conduction becoming more and more pronounced as the temperature is decreased toward the temperature of the phase transition (Figure 13).[25] While optical reflectance measurements under pressure allow us to discard the possibility of drastic changes in the band structure which evolves smoothly through the commensurabil-
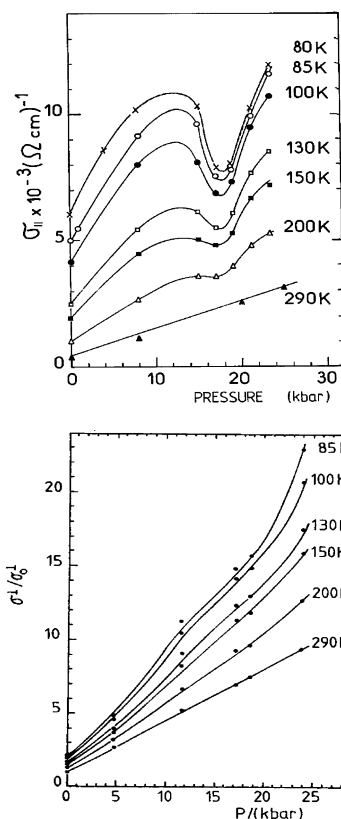
Figure 13. Pressure dependence of the conductivity of TTF−TCNQ showing the drop of metallic conductivity in the commensurability domain. The transverse conduction (bottom) remains unaffected by commensurability. (Reprinted with permission from ref 25. Copyright 1982 Taylor and Francis (http://www.tandf.co.uk/journals).)

ity domain,[55] the data in Figure 13 can be explained in the following two ways: (i) pinning of the rigid translation of fluctuating CDWs by commensurability effects or (ii) increase of the single particle scattering mechanism with the added possibility of a decreased density of states at the Fermi level in the commensurability domain. Fortunately, the transverse conductivity, as long as it is diffusive, is sensitive to both the density of states at the Fermi level and the smearing time $\tau_{\parallel}{}^{\text{sp}}$, leading to[57,58]

$$\sigma_{\perp} \approx N(E_{\text{F}})\tau_{\perp}{}^{-1} \qquad (2)$$

where $\tau_{\perp}{}^{\text{sp}}$ is the interchain hopping frequency given by

$$\frac{1}{\tau_{\perp}} = \frac{2\pi}{\hbar}|t_{\perp}|^2\tau_{\parallel}{}^{\text{sp}} \qquad (3)$$

and $t_{\perp}$ is the small interchain transfer integral. Consequently, eqs 2 and 3 lead to the relation

$$\sigma_{\perp} \approx N(E_{\text{F}})|t_{\perp}|^2\tau_{\parallel}{}^{\text{sp}} \qquad (4)$$

which is valid in the limit $\tau_{\perp} > \tau_{\parallel}{}^{\text{sp}}$ (i.e. for diffusive interchain conduction). This condition is met in TTF−TCNQ, since, according to NMR results, $\tau_{\perp}/\tau_{\parallel}{}^{\text{sp}} \approx 10^3$.[57] The data of transverse conductivity under pressure (Figure 13) failed to show any effect related to the commensurability domain. Consequently, we can be confident that the longitudinal conduction

data carry the signature for the suppression of a Fröhlich fluctuating component in the conduction which is present anywhere but in the commensurability domain. Some quantitative estimates of the fluctuating conduction have been performed in ref 25. They confirmed that the fluctuating contribution can be strongly suppressed by the third order commensurability while the single particle resistivity remains hardly affected. In this picture, the large contribution for the increase of the conduction between 300 and 60 K should be attributed to sliding conduction whereas the single particle does not increase more than a factor 2 or 3 in the same temperature range. Together with the results of X-ray scattering, which have localized the $2k_F$ lattice fluctuations of the 1D regime on the TCNQ stacks, the fluctuation conduction can be attributed to the TCNQ stack as well. Therefore, the large drop of spin susceptibility which is observed for the TCNQ stack by local susceptibility determination may be due to the opening of the pseudogap on the same stack. The attribution of the $4k_F$ scattering of the 1D regime to the TTF stack[48] suggests that this latter stack might be better described by a 1D electron gas with repulsive interactions in which charge and spin fluctuations are both gapless.[59,60] The decomposition of the conduction into two components has shown that the fluctuating part is hardly sensitive to pressure[56] (besides the suppression related to the commensurability domain). Therefore, the strong pressure dependence of the total conduction which is observed especially at high temperature must be ascribed to the single particle contribution enhanced by strongly pressure dependent correlation effects. The interplay between irradiation induced defects[61] and fluctuating conduction has also shown[56] that a value of 60 Å for the coherence length of the CDW fluctuations at 100 K is quite reasonable.

2.8. The Far-Infrared Response

This section will show how Fröhlich fluctuations are influencing the far-infrared spectrum of TTF–TCNQ. However, at first sight, the near-infrared optical studies with the light polarized along the most conducting axis revealed a Drude-like behavior over the entire temperature domain from 300 to 20 K, that is, covering both conducting and insulating regimes, with a plasma edge of about 7000 cm^{-1} and an optical scattering time $\tau \approx 2.3-310^{-15}$ s, which both do not show any significant temperature dependence.[62,63] Actually, plasma edge and scattering time both agree fairly well with the value of the dc conductivity at room temperature, $\sigma_{dc} = \omega_p^2 \tau/4\pi$. The finding of a plasma frequency which does not change throughout the whole range of temperatures is in agreement with the amplitude of the Peierls gap opening below 53 K being much smaller than the value of the plasma frequency itself. Subsequent studies performed in the insulating regime have pointed out the existence of several anomalies for the frequency dependent conductivity (Figure 14). The first is behavior typical of a semiconductor with an absorption edge around 300 cm^{-1} and second a sharp peak of conductivity at 35 cm^{-1}.[64] The broad absorption is the signature of the
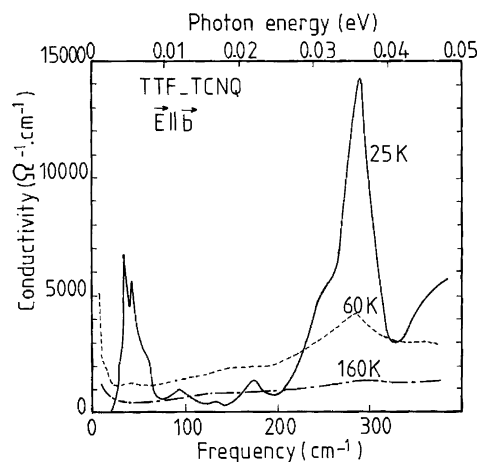
Figure 14. Far-infrared conductivity of TTF−TCNQ. (Reprinted with permission from ref 64. Copyright 1981 American Physical Society.)
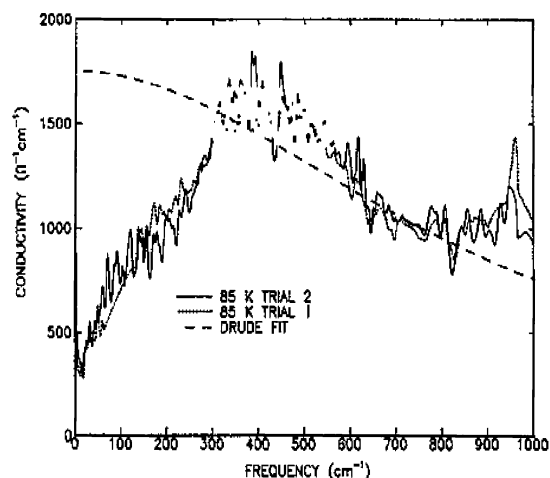
Figure 15. Far-infrared conductivity of TTF−TCNQ in the metallic regime. (Reprinted with permission from ref 60. Copyright 1990 American Physical Society.)

Peierls gap while the sharp feature was ascribed to the pinned CDW mode[65] or more likely to the oscillation of the hole density wave on TTF against the electron density wave on TCNQ.[60] Moving to the metallic regime, the pinned mode at finite frequency disappears but some gapping of the conductivity persists, although then the concept of a pseudogap appears to be more appropriate; see the data of Basista et al.[60] (Figure 15). This pseudogap in the metallic regime, still of the order of 300 cm^{-1}, has been ascribed to strong 1D fluctuations considering a 1D electron−phonon system without electron−electron interactions[43] and a mean field temperature of the order of 150 K. Since the frequency range is such that $\omega \ll \tau_{sp}$, the optical conductivity probes directly the density of states around the Fermi level. Figure 15 shows that the high frequency domain can be fitted rather well with a Drude conductivity using the parameters for the plasma frequency and the scattering time derived from the mid-infrared studies.[63] The low value of the conductivity, $\sigma \approx 400$ (Ω cm)$^{-1}$, at 20−50 cm^{-1} is in sharp contrast with the high dc conductivity observed at 60 K, $\sigma \approx 10^4$ (Ω cm)$^{-1}$. Furthermore, the missing oscillator strength in the pseudogap frequency regime is recovered in a

very narrow collective mode at zero frequency. Because of its very narrow width, the zero frequency collective mode cannot be easily detected in usual far-IR measurements. This mode can be described by a damped Drude-like mode with a conductivity σ_{coll} such as

$$\sigma_{coll} = \frac{\Omega_p^2 \tau_c}{4\pi(1 + \omega^2 \tau_c^2)} \qquad (5)$$

where Ω_p and τ_c are the plasma frequency and lifetime of the mode. These parameters can be obtained from the knowledge of the dc conductivity and from the frequency where the dielectric constant crosses zero, since $\epsilon_1(\omega) = \epsilon_H - \Omega_p^2/\omega^2$, where ϵ_H is the positive value of the dielectric constant at high frequency after it has crossed zero. A relaxation rate of $1/\tau_c = 4$ cm^{-1} has be obtained at 60 K by Tanner et al.[64] (although a much smaller value can be inferred from the work of Basista et al.,[60] $1/\tau_c = 0.05$ cm^{-1}). In addition, the collective mode of TTF−TCNQ has also been studied with the submillimeter spectroscopy[66] which provides direct access to the conductivity in the frequency range corresponding to the relaxation rate. It can thus be concluded from a comparison of the temperature dependence of σ at 10 cm^{-1} and at microwave frequencies (0.03−1 cm^{-1}) that the inverse lifetime lies between 1 and 10 cm^{-1}. In conclusion, the existence of a collective mode governing the dc conduction is firmly established from transport data when TTF−TCNQ is driven through commensurability by pressure and by the behavior of the far-IR and submillimeter conductivity, although a large uncertainty remains about the determination of its width. The far-IR data have also shown a large pseudogap in the single particle spectrum which is the counterpart of the collective mode. As $2k_F$ fluctuations in the metallic regime have been related to the TCNQ stacks,[48] it is very likely that these are the same fluctuations which are responsible for the depression of the density of states at the Fermi level and for the drop of the spin susceptibility of the TCNQ stacks[27] in the pseudogap regime.

2.9. Summary for TTF−TCNQ

TTF−TCNQ happens to be a particularly interesting 1D conductor which has profoundly marked the initial quest for superconductivity in organic compounds, although such an instability has not been found even using pressures up to 40 kbar, presumably because of the great stability of the Peierls transition which is further enhanced under pressure. What makes TTF−TCNQ fascinating is the existence of two parallel stacks which are only very weakly coupled by interchain hopping, unlike the case of single stack compounds pertaining to the (TM)$_2$X series, where the interstack coupling plays an important role in the physics at intermediate and low temperatures. Consequently, the conductivities of the two stacks are additive and can be modeled by two different physical pictures. Electron−phonon interactions are dominant on the TCNQ stack, where they are responsible for the 1D $2k_F$ CDW fluctuations seen

in X-ray scattering data and also for a large contribution to the dc conductivity peak at 60 K. The single particle spectrum of TCNQ is however strongly depressed by a pseudogap at the Fermi level of about 350 K opening below 150 K, thus providing a non-Drude behavior in the far-IR response with a lifetime for the narrow dc collective mode which is about 2 or 3 orders of magnitude longer than the single particle lifetime. It is also this pseudogap which governs the large temperature dependence of the TCNQ susceptibility.[27] Estimates for the contributions of the various conduction channels can be made at 60 K using the drop of conduction when CDWs fluctuations (on TCNQ stacks) can be pinned by commensurability effects under pressure; see ref 25. One would therefore obtain σ_{coll}(60 K) $\approx$ 5500 (Ω cm)$^{-1}$ and consequently σ_{sp}(60 K) $\approx$ 1500 (Ω cm)$^{-1}$. This latter value is in agreement with the optical conductivity of 1500 (Ω cm)$^{-1}$ measured in the frequency range 30−100 cm^{-1}, that is, at a frequency higher than the width of the collective mode,[67] and also with the loss of conduction occurring at the 53 K transition (which concerns only the stacks). On the other hand, electron−electron repulsions dominate the TTF stack. They provide $4k_F$ scattering and are responsible for a susceptibility which shows only a moderate decrease between 300 and 49 K, quite similar to the behavior of the susceptibility in (TM)$_2$X materials. The TTF stack can be viewed as an example of a Luttinger liquid in which charge and spin fluctuations are gapless.[59]

3. Selenide Molecules

In the 1970s the leading ideas governing the search for new materials likely to exhibit good metallicity and possibly superconductivity were driven by the possibility to minimize the role of electron−electron repulsions and at the same time to increase the electron−phonon interaction while keeping the overlap between stacks as large as possible. This led to the synthesis of a new series of charge-transfer compounds which went beyond the known TTF−TCNQ system, for example, changing the molecular properties while retaining the same crystal structure. It was recognized that electron polarizability was important to reduce the screened on-site e−e repulsion and that the redox potential $(\Delta E)_{1/2}$ should be minimized.[19,68] Hence, new charge-transfer compounds with TCNQ have been synthesized using other heteroatoms for the donor molecule, that is, substituting sulfur for selenium in the TTF skeleton, thus leading to the TSeF molecule $[(\Delta E)_{1/2} = 0.37$ eV for TTF and 0.32 eV for TSeF] and the synthesis of the charge-transfer compound TSeF−TCNQ. This compound has the same monoclinic structure as TTF−TCNQ, and the slight increase of the unit cell by 0.057 Å does not compensate for the significant increase of 0.15 Å for the van der Waals radius going from sulfur to selenium. Consequently, the cationic bandwidth of TSeF−TCNQ is increased by 28%, as shown by the tight binding calculation, while the TCNQ band is hardly affected.[54] It is probably the increase in the donor bandwidth with a concomitant decrease of the e−e repulsion on the TSeF stacks

which suppresses $4k_F$ fluctuations, *at variance* with TTF−TCNQ, where $4k_F$ scattering is observed from 300 K.[69] However, the observation of $2k_F$ scattering in TSeF−TCNQ below 230 K[69,70] prior to a Peierls transition at 29 K has led to an accurate determination of the incommensurate charge transfer, namely $\rho = 0.63$. As far as precursor structural effects are concerned, there are significant differences between TTF−TCNQ and TSeF−TCNQ. While precursor effects are 1D in TTF−TCNQ in almost the entire temperature domain where they are observed, the picture is different in TSeF−TCNQ, since short range 3D coupling is observed between 29 and 50 K and only limited 2D coupling is noticed up to 200 K.[71,70] Commensurability between CDWs and the underlying lattice (×3) has been detected at 6 kbar through a small peaking of the Peierls transition and a concomitant drop of the longitudinal conductivity.[72] The modest amplitude of the conductivity drop at commensurability suggests that the CDWs in the nonordered phase above 29 K are already partially pinned by transverse coupling and therefore cannot contribute dominantly to the fluctuating conduction of the metallic domain as for the case of TTF−TCNQ.[73]

The attempt to increase the transverse overlap and in turn stabilize a metallic phase at low temperature has been partly successful with the synthesis of new TCNQ charge-transfer compounds in which the structure exhibits a chessboardlike pattern. This is the case for hexamethylene-donor molecules with sulfur or selenium heteroatoms, HMTTF or HMTSF, respectively,[74,75] where metallicity is nearly achieved at low temperature. In HMTTF−TCNQ, an incommensurate CDW system with $\rho = 0.72$,[71] a semimetallic character can be maintained at low temperature under pressure above 19 kbar with $\delta\rho/\delta T > 0$, although a weak transition is still observed in resistivity at 30 kbar.[26] It was anticipated that the complete suppression of the distortion would require a pressure between 35 and 40 kbar. The selenide related compound HMTSF−TCNQ indicates a resistance minimum prior to a phase transition at $T_c = 24$ K,[76] which decreases under pressure but never vanishes in good quality samples.[25] This 24 K anomaly arises from the formation of a 3D superstructure corresponding to a charge transfer $\rho = 0.74$.[48] Thus, it was concluded that for HMTSF−TCNQ, due to the important deviation from planarity of the Fermi surface, the Peierls transition can only partly destroy it, so that the rest of the Fermi surface provides a semimetallic character to the compound at low temperature. This has been confirmed by the observation of quantum oscillations,[77] ruling out the early claim for the stabilization of a metallic state at helium temperature due to defective samples.[78]

The study of the two-chain charge-transfer compounds went on with a system where both donor and acceptor molecules had been methylated, namely, TMTSF−DMTCNQ (TM−DM), where the donor is the tetramethyl selenide derivative of TTF. The outcome of this study has been truly decisive for the quest of organic superconductivity.[79] This 1D conductor undergoes a Peierls transition at 42 K detected
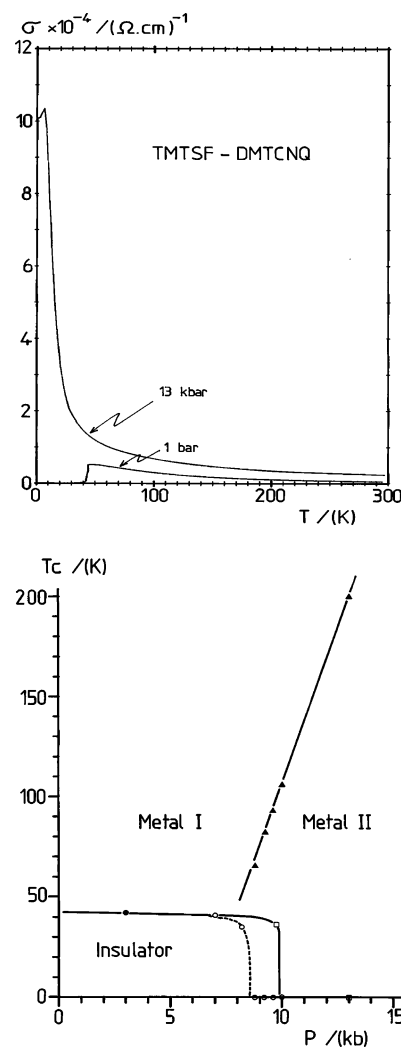
Figure 16. TMTSF−DMTCNQ: conductivity at ambient pressure and under 13 kbar (top) and $T−P$ phase diagram (bottom). (Reprinted with permission from ref 83. Copyright 1979 EDP Sciences.)

by conductivity[80] and magnetic[81] measurements where, unlike the case of TTF−TCNQ, a distortion occurs simultaneously on both chains.[82] Several other results have triggered the attention. X-ray experiments had shown that the charge transfer is only $\rho = 0.5$, leading to a quarter-filled band situation[82] for both acceptor and donor bands. Transport and thermopower data emphasized the dominant role played by the TMTSF chain in the mechanism driving the Peierls transition and also in its contribution to the conduction at high temperature.[81] The existence of a commensurability ×4 is in agreement with the only small increase of the conductivity upon cooling, peaking at a maximum of 5×10^3 $(\Omega$ cm$)^{-1}$ just above the metal−insulator transition, since fluctuative conduction is pinned by commensurability (×4) (Figure 16).

The pressure studies have shown that the commensurate state is fairly stable under pressure, since the Peierls transition remains at practically the same temperature of 42 K up to 8 kbar.[84] The really new and unexpected finding has been the suppression of the Peierls transition under a pressure of about 9 kbar and the conductivity remaining metal-like,
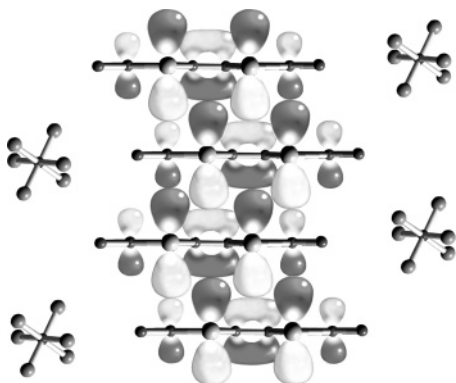
Figure 17. Side view of $(TM)_2X$ conductors.

reaching 10^5 $(\Omega$ cm$)^{-1}$ under 10 kbar at the temperature of liquid helium.[84] The stabilization of the conducting state at low temperature under pressure is actually related to a first-order pressure-driven phase transition between two different metallic phases. The conducting state of TM−DM was also remarkable in displaying a huge transverse magnetoresistance below 50 K when the magnetic field is aligned along the direction of weakest conduction. To explain such a large value for the conductivity at low temperature, the possibility of superconducting fluctuations enhancing the conduction was proposed despite the absence of any long range ordered superconducting state.[85] TM−DM is certainly an interesting system which should have deserved more work, but since all these phenomena were new and unexpected, the effort was put on a simpler structure made of only one organic stack comprising the lucky TMTSF molecule together with an inorganic monoanion which was able to reproduce the situation of a quarter-filled band. Such a structure was already known from the early work of the Montpellier chemistry group, who synthesized and studied the series of isostructural $(TMTTF)_2X$ organic salts,[86] where TMTTF is the sulfur analogue of TMTSF and X is a monoanion such as ClO_4^-, BF_4^-, or SCN^- and so forth; see Figure 1. All these compounds turned into strong insulators at low temperature and under atmospheric pressure. This is the reason they did not attract much interest until recently, when they have been revisited and made superconducting under pressure after twenty years of studies devoted mostly to the selenide series, $(TMTSF)_2X$.

4. The TM₂X Period

4.1. Organic Superconductivity in (TMTSF)₂X

In 1979, the Copenhagen group succeeded in the synthesis of a new series of conducting salts all based on the TMTSF molecule, namely, $(TMTSF)_2X$, where X is an inorganic anion with various possible symmetries: spherical (PF_6, AsF_6, SbF_6, TaF_6), tetrahedral (BF_4, ClO_4, ReO_4), or triangular (NO_3).[87] All these compounds but the one with X = ClO_4 did reveal an insulating ground state with a metal−insulator transition ranging from 180 K in X = ReO_4 down to 12 K in X = PF_6 (Figure 17). In this latter compound the conductivity reached the value 10^5 (Ω cm$)^{-1}$ at 12 K with still a very strong temperature
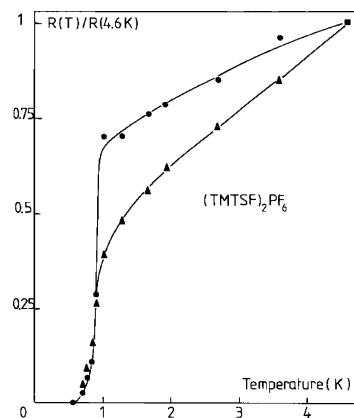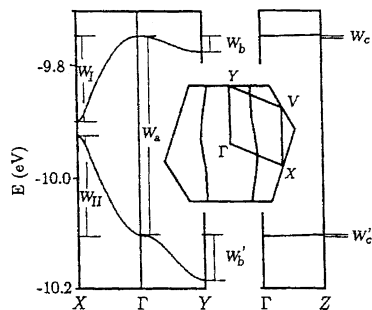

Figure 18. $(TMTSF)_2PF_6$: first observation of organic superconductivity (under a pressure of 9 kbar). (Reprinted with permission from ref 49. Copyright 1980 EDP Sciences.)

dependence. This behavior for the transport properties and the absence of any lattice modulation[82,88] as precursor to the metal−insulator transition were new features in this field still dominated by the CDW philosophy and stimulated further investigations under pressure and allowed the stabilization of a metallic state down to liquid helium temperature at a pressure of about 9 kbar. The finding of a very small and still nonsaturating resistivity at 1.3 K was a strong enough motivation to trigger further studies under pressure in a dilution refrigerator, which rapidly led to the discovery of a zero resistance state below 1 K. As this zero resistance state was easily suppressed by a magnetic field transverse to the most conducting direction, superconductivity was claimed.[49]

The discovery of superconductivity in the $(TMTSF)_2$-X family was a very exciting phenomenon, since it was the first time such an instability could be stabilized in an organic compound. This happened about 15 years after the publication of Little's suggestion and 10 years after the holding of an international symposium organized by W. A. Little in Hawai on the Physical and Chemical Problems of Possible Organic Superconductors.[10]

4.2. A Variety of Ground States in the (TM)₂X Series

The discovery of superconductivity in an organic conductor triggered subsequent investigations of the $(TMTSF)_2X$ series, which have shown that the superconducting ground state is only one among a variety of other ground states which can be stabilized in the isostructural series depending either on the nature of the anion or on the applied pressure. Shortly after the discovery of superconductivity in $(TMTSF)_2PF_6$ (Figure 18) it was realized that the mechanism driving the metal−insulator transition at 12 K in $(TMTSF)_2PF_6$ at ambient pressure is the onset of itinerant antiferromagnetism, which sets a magnetic modulation called a spin density wave (SDW). SDW formation had been proposed earlier for the interpretation of the magnetic transition in chromium due to the nested regions of the peculiar Fermi surface of this 3D metal.[89,90] However, what makes the onset of a SDW particularly damaging for

Figure 19. Band structure and Fermi surface of $(TMTSF)_2PF_6$. (Reprinted with permission from ref 91. Copyright 1994 EDP Sciences.)
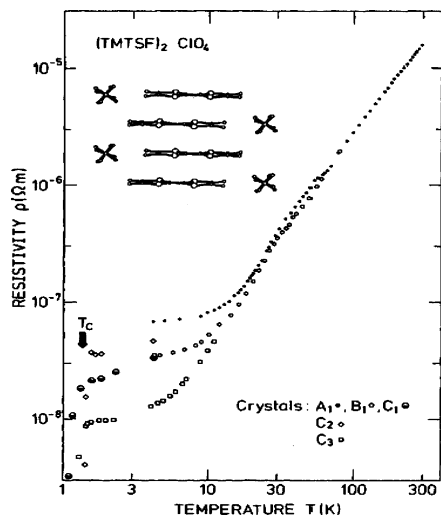
**Figure 20.** $(TMTSF)_2ClO_4$: first observation of organic superconductivity at ambient pressure. (Reprinted with permission from ref 93. Copyright 1981 American Physical Society.)

a 1D conductor like $(TMTSF)_2PF_6$ is the planarity of the Fermi surface. With a band filled up to $\pm k_F$ the exchange term of the Hartree−Fock potential characterized by the wave vector $2k_F$ in the SDW phase opens a gap at the Fermi level over the entire surface, giving rise in turn to an insulating ground state.

Shortly after the discovery of superconductivity in $(TMTSF)_2PF_6$, many other members of the same series with a variety of anions were also found to be superconducting in the vicinity of 1 K in the 10 kbar pressure domain.[92] However, $(TMTSF)_2ClO_4$ is the only member of the $(TMTSF)_2X$ series to show superconductivity under atmospheric pressure (Figure 20).[93] In the mid-1980s, the isostructural family comprising the sulfur molecule (TMTTF) with the same series of monoanions was investigated under pressure, and quite interesting new results were obtained.[94] Thanks to studies performed at higher pressures, it was realized that $(TMTTF)_2X$ and $(TMTSF)_2X$ salts both belong to the same family, forming the generic $(TM)_2X$ phase diagram[95] (Figure 21).

At this stage, it is instructive to look at the band structure, which can be foreseen for these materials on the basis of a single particle model using a tight binding scheme and few simplifications. One is the use of the highest occupied molecular orbital (HOMO) as the starting wave function for the TB calculation,
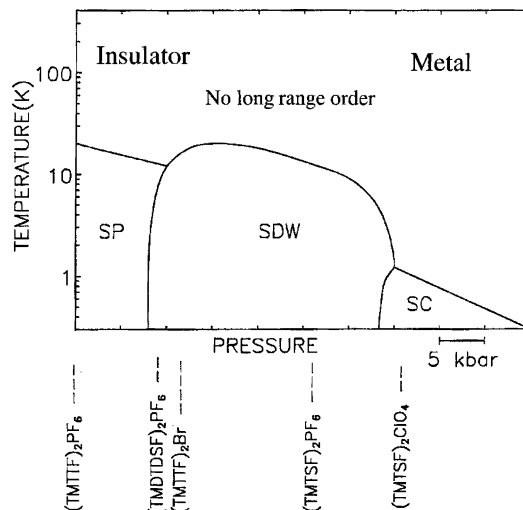
Figure 21. Generic phase diagram for the $(TM)_2X$ compounds. (Adapted with permission from *Science* (http://www.aaas.org), ref 95. Copyright 1991 American Association for the Advancement of Science.)

which is jusified by the only weak interaction existing between molecules in the solid state. The other is the extended Hückel method, which leads to an appropriate band description.

The band structure parameters thus obtained can be used to define the following model of the energy spectrum:[25,96]

$$\epsilon(\vec{k}) = -2t_a \cos(k_a a/2) - 2t_{\perp b} \cos(k_{\perp b} b) - \\ 2t_{\perp c} \cos(k_{\perp c} c) \quad (6)$$

where it is assumed that the underlying lattice is orthorhombic. With the symmetry of the lattice in the $(TM)_2X$ being triclinic with the $P\bar{1}$ space group, the above expression then represents a simplified model of the actual spectrum of Figure 19, but it retains the essential points and is easier to manipulate. The conduction band along the chain direction has an overall width $4t_a$ ranging between 0.4 and 1.2 eV, depending on the chemical nature of the donor molecule. As the overlap between electron clouds of neighboring molecules along the stacking direction is about 10 times larger than the overlap between the stacks in the transverse b direction and 500 times larger than that along the c direction, the electronic structure can be viewed at first sight as one-dimensional with an open and slightly warped Fermi surface centered at the Fermi wave vector $\pm k_F$ defined for isolated chains (Figure 19).

The anions located in centrosymmetrical cavities lie slightly above or below the molecular planes. This structure results in a dimerization of the intermolecular distance (overlap) with a concomitant splitting of the HOMO conduction band into a filled lower band separated from a half-filled upper (holelike) band by a gap Δ_D at $\pm 2k_F$, called the dimerization gap, which is shown in Figure 22 at the point X of the new Brillouin zone. However, on account of the finite transverse dispersion, this dimerization gap does not lead to a genuine gap in the middle of the density of states, as shown from the extended Hückel band calculation (Figure 22). The only claim which
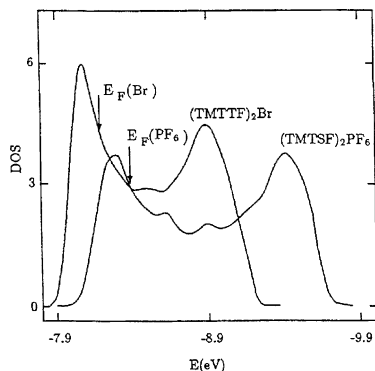
Figure 22. Extended Hückel density of states for $(TMTSF)_2PF_6$ and $TMTTF_2Br$. (Reprinted with permission from ref 91. Copyright 1994 EDP Sciences.)

Table 1. Calculated Band Parameters for Three Representative Members of the $(TM)_2X$ Series According to the Room Temperature Crystallographic Data in Ref 97[a]

	$(TMTTF)_2PF_6$	$(TMTSF)_2PF_6$	$(TMTSF)_2ClO_4$
t_1	137	252	258
t_2	93	209	221
$\bar{t}$	115	230	239
$\Delta t/\bar{t}$	0.38	0.187	0.155
$\bar{t}_\perp$	13	58	44

[a] The average intra- and interstack interactions are given in lines 3 and 5, respectively. The bond dimerization is shown in line 4. All energies are in millielectronvolts.

can be made is that these conductors have a commensurate band filling (0.75) coming from the 2:1 stoichiometry with a tendency toward half filling which is more pronounced for sulfur (with enhanced structural dimerization) than for selenium compounds, while it differs from compound to compound within a given series. Consequently, according to the single particle band calculation, all compounds in the $(TM)_2X$ series should be found to be conducting. In Table 1 we report the band parameters of different members of the $(TM)_2X$ family, as they can be computed from the crystallographic data.[97] The sulfur compounds exhibit bands which are significantly narrower and more dimerized than the selenide ones. The compound $(TMTTF)_2Br$ (not listed in Table 1) is however an exception among sulfur compounds with a dimerization of 0.13, smaller than the value calculated for $(TMTSF)_2ClO_4$. This might possibly be due to a calculation of the electronic bands based on rather old crystallographic data and less accurate data than those of the other compounds.[98] If the small band dimerization of $(TMTTF)_2Br$ is indeed right, this would support the claims made in section 4.8 for the predominance of the Umklapp scattering in a quarter-filled band as the cause for electron localization in the $(TM)_2X$ series.

The gross features of the $(TM)_2X$ phase diagram are the following. First, compounds on the left in the diagram, such as $(TMTTF)_2PF_6$, are insulators below room temperature while those to the right of $(TMTTF)_2Br$ exhibit an extended temperature regime with a metallic behavior; see Figure 23. Therefore, the cause for the insulating nature of some members in the $(TM)_2X$ series will have to be researched in the
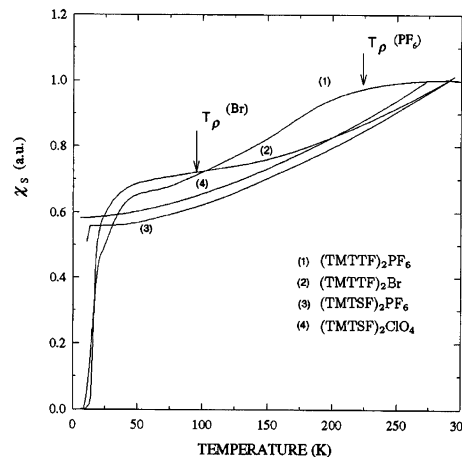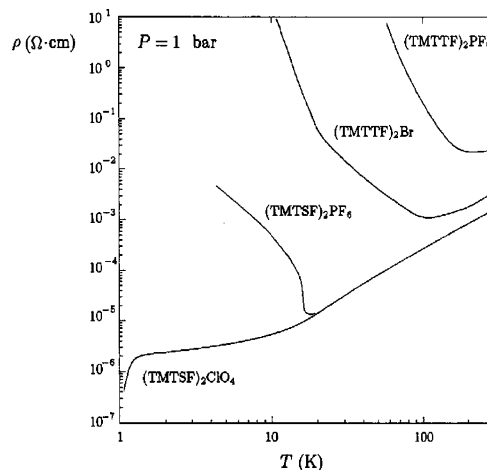
Figure 23. $(TM)_2X$: resistivity and susceptibility. An illustration for the charge−spin separation. (Reprinted with permission from ref 100. Copyright 1999 Elsevier.)

joint role of e−e repulsion and low dimensionality, as we shall show later on in this review.

The salient feature of the $(TM)_2X$ diagram is the existence of a wide variety of ground states occurring below 20 K or so. Moving toward the right across the $(TM)_2X$ phase diagram, a succession of ground states is revealed with either changing compounds or changing pressure on a given compound. All these ground states have been discovered from the study of the temperature dependence of the spin degrees of freedom (susceptibility, EPR, and NMR) and from structural data.[99] The compound at the extreme left in the $(TM)_2X$ diagram, $(TMTTF)_2PF_6$, is the only one which can be moved by pressure through the entire series of ground states—spin−Peierls, Néel antiferromagnetism, and SDW phase—with an incommensurate magnetic modulation and ultimately superconductivity. It is this latter compound which has settled the universality of the generic phase diagram.[95]

4.3. Charge Ordering in the Insulating State of $(TMTTF)_2X$

The dominant role of Coulomb interactions between one-dimensional carriers of these salts has been illustrated by the observation of a new electronic state detected a long time ago in the $(TMTTF)_2X$ members of the $(TM)_2X$ series but understood only

recently: the charge-ordered (CO) state. The early evidences came from the study of the transport properties, showing sharp anomalies of resistivity, thermopower,[101] and microwave dielectric constant[102] in the salts with X = SbF$_6$, AsF$_6$, and ReO$_4$ of the (TMTTF)$_2$X family at T_{CO} = 154, 100, and 225 K, respectively. In addition, it had been noticed that none of these anomalies were accompanied by structural modifications, and thus, the name "structureless transitions" was given to them.[103] Similarly, the absence of any change of the spin degrees of freedom was taken as an evidence for the spin–charge separation of the 1D electron gas physics, but the actual understanding of these features came only recently with the investigation of local properties with NMR studies.[104,105] The NMR measurements ascribed the anomalies at T_{CO} to the existence of an electronic phase transition and the onset of a charge disproportionation occurring between near neighbor molecules along the molecular stacks. As shown by the splitting of the NMR lines,[104] the charge redistribution removes the inversion symmetry $P\bar{1}$ existing at high temperature and gives rise to a modulation at wave vector $4k_F$ of the molecular site energy, leading in turn to an additional increase of the preexisting charge gap due to on-site correlations and Umklapp scattering[106] (vide infra). The CO transition is also accompanied by the onset of a ferroelectric state, which has been revealed by the divergence of the low frequency dielectric constant.[107,108] The case of (TMTTF)$_2$SbF$_6$ is indeed quite peculiar, as it is a metal–insulator transition which is observed at T_{CO} instead of the usual insulator–insulator transition with a concomitant increase of the activation energy observed in all other compounds such as (TMTTF)$_2$-AsF$_6$[108] and even in (TMTTF)$_2$BF$_4$ recently.[109] The strengthening of the dimerization gap (and in turn of the localization) has been anticipated in two different theoretical approaches. It was first shown from numerical calculations of the 1D extended Hubbard model that the nearest neighbor interaction V added to the on-site repulsion U resulted in a CDW singularity at $4k_F$.[110] Subsequently, the calculation of the ground state of a quarter-filled 1D band within a mean field approximation of the extended Hubbard chain[111] showed how the long range part of the Coulomb interaction is essential to stabilize a charge disproportionated state (leaving the spin excitations unaffected). As 1D correlations only are unable to explain long range order and the existence of finite temperature phase transitions, a uniform displacement of the anion lattice has been suggested as the 3D stabilizing agent[108] leading to a ferroelectric ground state[112] through the second-order transition where the permittivity is found to be diverging with a Curie law.[108] High pressure studies have shown that the CO state survives the formation of the spin-singlet (spin–Peierls) ground state and may coexist with it in a narrow pressure domain,[105] in agreement with the 1D extended Hubbard calculation adding the electron–lattice coupling.[113] In conclusion, the phenomenon of charge ordering observed in practically all members of the (TMTTF)$_2$X subfamily has emphasized the importance of the long range Coulomb
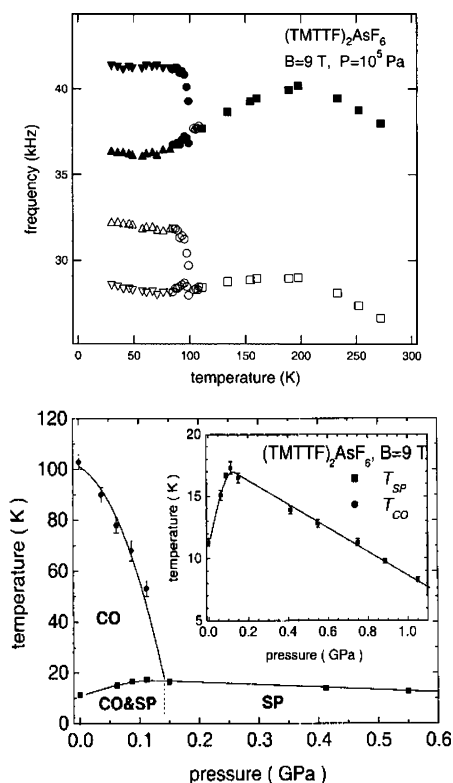
Figure 24. (TMTTF)$_2$AsF$_6$: Knight shift data showing the onset of charge disproportionation below 100 K (top) and P–T phase diagram (bottom). (Reprinted with permission from ref 105. Copyright 2002 EDP sciences.)

interactions besides on-site repulsions. The fast suppression under pressure (see Figure 24) is also suggestive of a rather modest influence on the properties of the more metallic compounds which become superconducting at low temperature. The phenomenon of charge ordering is not restricted to salts with centrosymmetrical anions, but in the case of the tetrahedral anion ReO$_4$, charge ordering is observed at a first transition with T_{CO} = 225 K (the structureless transition) and it is followed at lower temperature by an anion ordering transition at T_{AO} = 154 K (see next section) leading to a superstructure ($\frac{1}{2}$, $\frac{1}{2}$, $\frac{1}{2}$) and an increase of the activation energy.[101,102]

4.4. Symmetry of the Anions

Although most of the physics of organic conductors is governed by the organic molecules, the anions, the presence of which is essential for electric neutrality, may in some case suppress the stability of the conducting phase. As a matter of fact, the possibility for (TM)$_2$X compounds having non-centrosymmetrical anions to undergo a structural phase transition can modify the band structure and the topology of the Fermi surface. Anions such as ClO$_4$, ReO$_4$, NO$_3$, SCN, and FSO$_3$ have two equivalent orientations corresponding to short and long contacts between the Se (respectively S) atoms of the TMTSF (respectively TMTTF) molecule and a peripheral electronegative atom of the anion. Consider the case of (TMTSF)$_2$ClO$_4$: the anion lattice orders at 24 K, leading to a superstructure of the Se–O contacts with a wave vector $\mathbf{q}_A$ = (0, $\frac{1}{2}$, 0) here expressed in units of the

reciprocal lattice vector.[106,114] The periodic potential thus created connects two Fermi points along the b direction and opens a gap which doubles the unit cell along that direction. The folding of the Fermi surface that results introduces two warped Fermi surfaces near $\pm k_F$. Anion lattice superstructure has thus important consequences on the one-particle spectrum and in particular the nesting properties of the Fermi surface. This plays an important role in the efficiency of electron−electron interactions at low temperature and in the nature of the ground states. It also controls the stability of the superconducting phase in (TMT-SF)$_2$ClO$_4$ below 1.2 K at ambient pressure when the long range orientation is defective. The variety of features induced by a magnetic field, such as the so-called quantization of the Fermi surface nesting in the spin density wave phase ordering, namely, field induced spin density wave (FISDW) phases[115−120] and the Lebed resonances,[121] is also sensitive to the symmetry of the anions. This is particularly manifest when it is compared to compounds with spherical anions such as PF$_6$, AsF$_6$, and so forth, for which the absence of alteration of the Fermi surface via anion ordering entails, for example, the stabilization of spin density wave long range order in zero magnetic field at ambient pressure.

For other compounds with a non-centrosymmetrical anion like ReO$_4$, the structural ordering is different and takes place at $\mathbf{q}_A = (^1/_2, ^1/_2, ^1/_2)$; its impact on the electronic structure, however, turns out to be more marked, since the anion potential at this wave vector creates a gap over the whole Fermi surface which is so large in amplitude ($\sim t_a$) that it leads to an insulating state in which electron−electron interactions probably play little role. The application of hydrostatic pressure is then required to restore the metallic state and the possibility of long range ordering for electronic degrees of freedom.[123,124]

As previously mentioned, the anion potential produced by spherical anions such as PF$_6$, AsF$_6$, and so forth leads to a modulation of the charge along the organic stack with the same periodicity as the dimerization.[125] It may independently contribute to the half-filled character of the band and then enhance the strength of the electron−electron interaction at low temperature.[126]

4.5. Some Features of the Superconducting State

We shall not talk about the detailed features of the insulating (spin−Peierls or magnetic) ground states of the (TM)$_2$X diagram which can be found in various reference articles and textbooks[127] but shall devote a few words about a discussion of the superconducting state, which remains the flagship of the (TM)$_2$X story.

4.5.1. The Superconducting Transition

We intend to review briefly some physical features related to the onset of the superconducting state in (TMTSF)$_2$X, limiting ourselves only to some of the experiments which have been used to characterize this state. The observation of superconductivity in the (TMTTF)$_2$X series requires the extended use of high pressure,[92,128] with the notable exception of
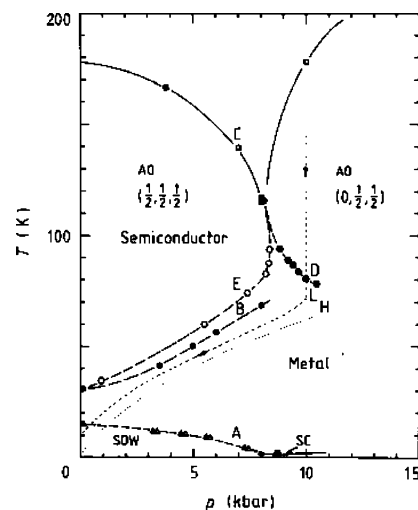
Figure 25. (TMTSF)$_2$ReO$_4$: phase diagram displaying the SDW ground state obtained after the "Orsay process". (Reprinted with permission from ref 124. Copyright 1989 Institute of Physics).

(TMTSF)$_2$ClO$_4$, which is superconducting under ambient pressure,[93] and (TMTSF)$_2$NO$_3$, which never becomes a superconductor even under pressure.[129] For all cases the first evidence for superconductivity has been provided by a drop of the resistivity below the critical temperature and the suppression of this drop under magnetic field. We shall focus the presentation on the two members of the (TMTSF)$_2$X series which have attracted most attention: (i) (TMTSF)$_2$PF$_6$, because this has been the first superconductor to be found by transport measurements[49] and confirmed by magnetic shielding[130,131]and also because the electronic properties of the 1D electron gas on the organic stacks are only weakly (if at all) affected by the centrosymmetrical anions, and (ii) (TMTSF)$_2$ClO$_4$, because it is the only member on which some experiments such as specific heat[132] or Meissner expulsion[133] have been performed.[133,134] However, the study of the superconducting state in (TMTSF)$_2$ClO$_4$ is meeting the problem of the ClO$_4$ anions ordering at 24 K doubling the periodicity along the b-axis.[135] Consequently, great care must be taken to cool the sample slowly enough to reach a well ordered state (R state) at low temperature; otherwise, superconductivity is faced with its great sensitivity to disorder, which will be discussed below. The limitation for (TMTSF)$_2$PF$_6$ is quite different. It is the proximity under pressure between SDW and superconducting phases which prevents the study of an homogeneous superconducting state unless the pressure is far above the critical pressure suppressing the SDW phase (vide infra). The specific heat of (TMTSF)$_2$ClO$_4$ in a C/T versus T plot (Figure 26) displays a very large anomaly around 1.2 K.[132] Above 1.22 K, the specific heat obeys the classical relation in metals: $C/T = \gamma + \beta T^2$, where $\gamma = 10.5$ mJ mol^{-1} K^{-2}, corresponding to $N(E_F) = 2.1$ states eV^{-1} mol^{-1} for the two spin directions. The specific heat jump at the transition amounts then to $\Delta C/\gamma T_c = 1.67$, that is, only slightly larger than the BCS ratio. The behavior of $C(T)$ in the superconducting state leads to the determination of the thermodynamical critical field $H_c = 44 \pm 2$ Oe and the single particle gap 2Δ
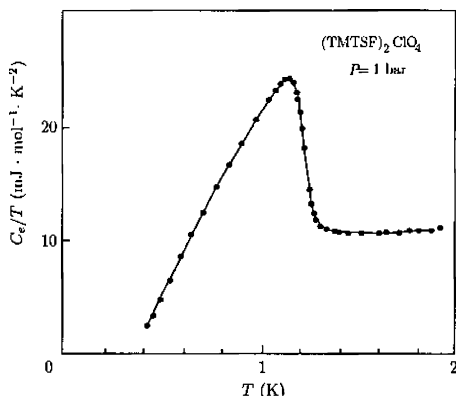
Figure 26. (TMTSF)$_2$ClO$_4$: C/T versus T. (Reprinted with permission from ref 132. Copyright 1982 American Physical Society.)

= 4 K. T_c is depressed at a rate of 1.1 mK/Oe^{-1} when a magnetic field is applied along the c^*-axis.[136] Comparing the value of the density of states derived from the specific heat and the value of the Pauli susceptibility[137] lends support to a weak coupling Fermi liquid picture (at least in the low temperature range).[100] The anisotropic character of the electronic structure already known from the anisotropy of the optical data in the normal phase is reflected in a severe anisotropy of the critical fields H_{c2} measured along the three principal directions in (TMTSF)$_2$ClO$_4$.[134,138-140] The linearity of the critical fields with temperature in the vicinity of T_c suggests an orbital limitation in the Ginzburg−Landau formalism for the critical field and rules out a Pauli limitation which would favor a $(1 - T/T_c)^{1/2}$ dependence.[138,141] However, the a/b anisotropy measured from critical fields is at least a factor of 2 below the anisotropy derived from plasma edge studies. The interpretation of the critical fields in (TM)$_2$X is still waiting for an answer, since several experimental results seem to imply that critical field values could overcome the Pauli limit at low temperature by factors of 2 or more.[142,143] Here too, great care must be taken to measure the critical field in an homogeneous superconducting phase, as will be presented in section 4.5.4.

4.5.2. Superconductivity under Pressure

The pressure dependence of T_c is admittedly a remarkable feature for the (TM)$_2$X compounds, since it is pressure which enabled organic superconductivity to be discovered. As far as (TMTSF)$_2$PF$_6$ is concerned, the strong pressure dependence observed above 10 kbar (T_c is only 0.2 K under 24 kbar[144]) leads to a Gruneisen constant $\delta \ln T_c/\delta \ln T = 11$ at 9 kbar,[144] and using the compressibility data at 16 kbar[145] gives $\delta \ln V/\delta P = 0.7\%$ kbar^{-1}. This value of 11 is indeed larger than what has been derived for tin (7), the classical superconductor which reveals the strongest sensitivity to pressure. The stability of superconductivity in (TMTSF)$_2$ClO$_4$ is even more dramatic, since then $\delta \ln T_c/\delta \ln T = 36$[146] using the compressibility of 1% kbar^{-1} measured for (TMTSF)$_2$PF$_6$ at ambient pressure.[145] However, this remarkable sensitivity of T_c in ClO$_4$ might actually be related to the very specific problem of anion ordering in this compound, as has been suggested from the recent

study of the sensitivity of T_c against the presence of nonmagnetic disorder.[147] Anion ordering reveals an uprise of the ordering temperature under pressure[146,148,149] which can be derived from the pressure dependence of a small kink in the resitivity, the signature of the ordering, moving from 24 up to 26.5 K under 1.5 kbar. Together with this uprise there exists a slowing down in the dynamics of the anions needed for the ordering. Hence, high pressure studies require special attention to the cooling rate, which must be kept low enough to allow anion ordering at low temperature. This may be the explanation for the discrepancy between high pressure data showing the signature of anion ordering up to 8 kbar[149] and the absence of ordering claimed from the interpretation of magnetoangular oscillations.[150]

4.5.3. Superconductivity and Nonmagnetic Defects

It is also the remarkable sensitivity of organic superconductivity to irradiation[151,152] which led Abrikosov to suggest the possibility of triplet pairing in these materials.[153] Although irradiation was recognized to be an excellent method for the introduction of defects in a controlled way,[154] defects thus created can be magnetic,[155] and the suppression of superconductivity by irradiation induced defects as a signature of nonconventional pairing must be taken with "a grain of salt", since local magnetic moments can also act as strong pair-breakers on s-wave superconductors. Several routes have been followed to introduce an intrinsically nonmagnetic perturbation modulating the potential seen by the carriers on the organic stacks. Substituting TMTTF for TMTSF on the cationic stacks of (TM)$_2$X salts, non-disorder has been achieved with PF$_6$[94] and ClO$_4$ salts.[156] However, in both situations, cationic alloying induces drastic modification of the normal state electronic properties, since the SDW transition of (TMTSF)$_2$PF$_6$ is quickly broadened and pushed toward higher temperature upon alloying.[157]

Leaving the cation stack uniform, scattering centers can also be created on the anion stacks with the solid solution (TMTSF)$_2$(ClO$_4$)$_{(1-x)}$(ReO$_4$)$_x$, where Tomić et al. first mentioned the suppression of superconductivity upon alloying with a very small concentration of ReO$_4$ anions.[158] In the case of a solid solution with tetrahedral anions such as ClO$_4$ or ReO$_4$, one is confronted with two potential sources of nonmagnetic disorder which act additively on the elastic electronic lifetime according to Mathiessen's law: first the modulation due to the different chemical natures of the anions and second a disorder due to a progressive loss of long range ordering at T_{AO} in the (TMTSF)$_2$(ClO$_4$)$_{(1-x)}$(ReO$_4$)$_x$ solid solution although X-ray investigations have revealed that long range order is preserved up to 3% ReO$_4$ with a correlation length $\xi_a > 200$ Å.[159] Studies of superconductivity in (TMTSF)$_2$(ClO$_4$)$_{(1-x)}$(ReO$_4$)$_x$ conducted under extremely slow cooling conditions have shown that T_c is a fast decreasing function of the nonmagnetic disorder[147] where the residual resistivity along the c^*-axis has been used for the measure of the disorder in the alloys with different concentrations, (Figure 27). The suppression of T_c must be related to the enhancement
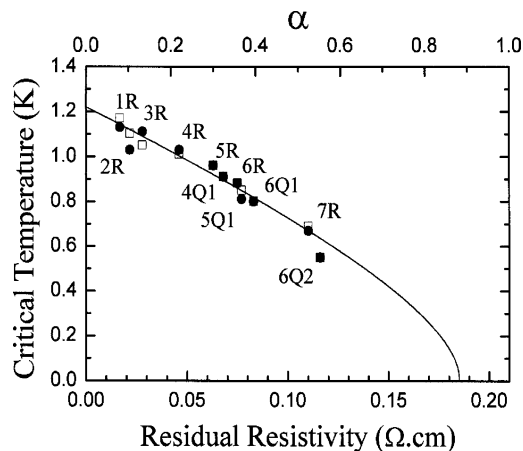
Figure 27. Superconducting critical temperature as a function of the residual resistivity for samples with different amounts of disorder, either chemical (nR) or orientational (nQ). The solid line is a least-squares fit of the digamma pair-breaking function to the data which reaches zero at α = 0.88. (Reprinted with permission from ref 147. Copyright 2004 EDP Sciences.)

of the scattering rate in the solid solution. Since the additional scattering cannot be ascribed to magnetic scattering according to the EPR checks showing no additional traces of localized spins in the solid solution, the data in Figure 27 cannot be reconciled with the picture of a superconducting gap keeping a constant sign over the whole ($\pm k_F$) Fermi surface. They require a picture of pair-breaking in a superconductor with an unconventional gap symmetry. The conventional pair-breaking theory for magnetic impurities in usual superconductors has been generalized to the case of nonmagnetic impurities in unconventional materials, and T_c reads[160,161]

$$\ln\left(\frac{T_{c0}}{T_c}\right) = \Psi\left(\frac{1}{2} + \frac{\alpha T_{c0}}{2\pi T_c}\right) - \Psi\left(\frac{1}{2}\right) \qquad (7)$$

with Ψ being the digamma function, $\alpha = \hbar/2\tau k_B T_{c0}$ the depairing parameter, τ the elastic scattering time, and T_{c0} the limit of T_c in the absence of any scattering. From the data in Figure 27 the best fit leads to T_{c0} = 1.22 K and a critical scattering for the suppression of superconductivity of $1/\tau_{cr}$ = 1.44 cm^{-1}, τ_{cr} = 3.5 ps (following the definition of α). Accordingly, $1/\tau$ amounts to 0.13 cm^{-1} (τ = 40 ps) in the pristine (TMTSF)$_2$ClO$_4$ sample. The sensitivity of T_c to nonmagnetic disorder cannot be reconciled with a model of conventional superconductors. The gap must show regions of positive and negative signs on the Fermi surface which can be averaged out by a finite electron lifetime due to elastic scattering. As these defects are local, the scattering momentum of order $2k_F$ can mix $+$ and $- k_F$ states and therefore the sensitivity to nonmagnetic scattering is still unable to tell the difference between p or d orbital symmetry for the superconducting wave function. A noticeable progress could be achieved by paying attention to the spin part of the wave function. In the close vicinity of T_c, orbital limitation for the critical field is expected to prevail, and therefore, the analysis of the critical fields close to T_c[141] does not necessarily imply a triplet pairing. When the magnetic field is oriented along the inter-

mediate b-axis, violations of the Pauli limitation have been claimed in the (TMTSF)$_2$PF$_6$[142] and, recently, (TMTSF)$_2$ClO$_4$[143] superconductors. However, it must be kept in mind that in all these experiments under transverse magnetic field the electronic structure is profoundly affected by the application of the field, which tends to localize the electrons, as shown by the enormous magnetoresistance in the normal state. Furthermore, it is still unclear whether the superconducting phase remains homogeneous under a strong transverse field.[162,163] Older data in (TMTSF)$_2$-ClO$_4$[140] are not in contradiction with the picture of singlet pairing, but no data were given below 0.5 K, the temperature domain where it would be most rewarding to see how H_{c2} compares with the Pauli limit when H is perfectly aligned along the a-axis. The nature of the superconducting coupling in (TM)$_2$X conductors is still intensively studied and debated. The absence of temperature dependence of the ^{13}C Knight shift through the critical tempeature at a pressure where (TMTSF)$_2$PF$_6$ is superconducting[164] implies a triplet pairing. However, the sample thermalization during the time of the NMR experiment has been questioned,[165] and this result will have to be reconfirmed. Researchers have not yet reached a consensus about the nature of the coupling in (TM)$_2$X superconductors. This is due in part to the lack of unambiguous experimental data for samples exhibiting superconductivity in the very low temperature region. This is *at variance* with the singlet coupling found in 2D organic superconductors with a T_c in the 10 K range, as clearly indicated by the Knight shift measurements in the superconducting state.[166,167] It can be noticed that, despite the established singlet coupling, the critical fields H_{c2} of 2D superconductors can also exceed the paramagnetic limit in the parallel geometry.[165,168,169]

4.5.4. Inhomogeneous Superconductivity

Situations for nonhomogeneous superconductivity have been clearly identified near the border between the SDW and superconductivity in the (TM)$_2$X phase diagram (Figure 28).[170] At high pressure ($P >$ 9.4 kbar) the superconducting phase emerges from a metallic state and can be reasonably thought as homogeneous with a critical current density along the a-axis J_c = 200 A·cm^{-2}, while below this critical pressure there exists a pressure domain ($\approx$1 kbar wide) in which superconducting features are observed at a pressure independent temperature below the onset of a SDW instability where the critical current density is greatly reduced, $J_c \approx$ 10 A·cm^{-2}. This points in favor of a coexistence of SDW and SC macroscopic domains (Figure 28). A related consequence of the existence of macroscopic insulating domains in the superconducting phase allowing a channeling of the lines of force in the material is a large increase of the upper critical field H_{c2},[171] which had already been reported a long time ago in (TMTSF)$_2$PF$_6$,[172] for the first repetition of organic superconductivity, and also (TMTSF)$_2$AsF$_6$.[173] Recent data obtained with (TMTTF)$_2$PF$_6$ under very high pressure have clearly shown that the critical field for $H\|c^*$ is enhanced by a factor 10 at the border with the SDW phase, where it can reach 1 T, while it amounts
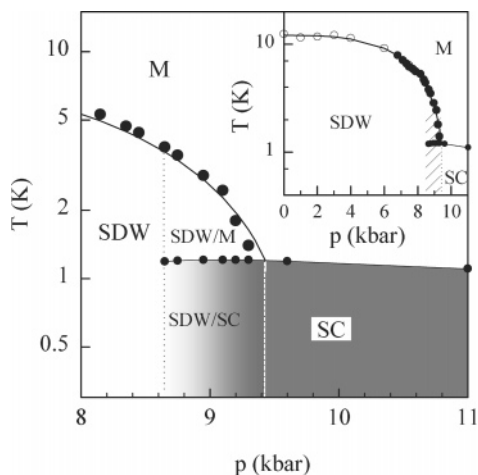
Figure 28. Coexistence between SDW and superconductivity in $(TMTSF)_2PF_6$ in the vicinity of the criticial pressure for suppression of the SDW ground state. (Reprinted with permission from ref 170. Copyright 2002 EDP Sciences.)

to <0.1 T at very high pressure when the superconducting state is homogeneous,[174] a value similar to the observation in the R state of $(TMTSF)_2ClO_4$. It must be kept in mind that the slab formation in the vicinity of the SDW state with the formation of insulating domains is not related to the penetration of the magnetic field in a type II superconductor but is the result of a competition between insulating and conducting phases.

4.6. $(TM)_2X$: From the 1D Mott Insulator to the 2D Conductor

Given the unified $(TM)_2X$ phase diagram established experimentally which suggests that apparently so different systems such as the superconducting $(TMTSF)_2ClO_4$ and the strongly insulating $(TMTTF)_2PF_6$ belong to the same class of materials, that is, the physical properties of the latter can be made equivalent to those of the former provided a large enough pressure is applied, we shall try to explain how recent theoretical ideas in 1D physics have contributed to a better understanding. Therefore, we intend to summarize very briefly the physics of the high temperature phase in the rest of this article. Extended reviews have been published in ref 100 and also in a recent textbook.[175]

What 1D physics means is that, instead of the usual description of low lying excitations in terms of quasi particle states in the Landau−Fermi liquid model, a collective mode description with decoupled spin and charge modes is a more appropriate starting point.[176,177] Such a model for 1D conductors has been proposed starting from a linearized energy spectrum for excitations close to the Fermi level and adding the relevant Coulomb repulsions which are responsible for electron scattering with momentum transfer $2k_F$ and 0. This is the popular Tomonaga−Luttinger model for a 1D conductor in which the spatial variation of all correlation functions (spin susceptibility at $2k_F$ or $4k_F$, CDW, superconductivity) exhibits a power law decay at large distance, characterized by a nonuniversal exponent K_ρ (which is a function
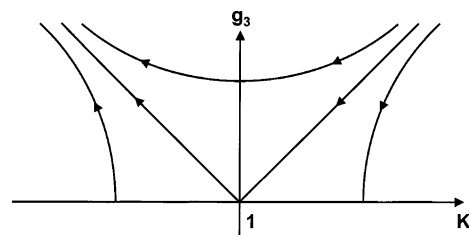

Figure 29. Temperature flow of interactions g_3 (Umklapp scattering amplitude) and K_ρ for the half-filled band situation.

of the microscopic coupling constants).[178] This experimental review is not the place to discuss extensively the significance of the 1D exponent, but let us just say, to be extremely brief, that K_ρ is a positive exponent. When K_ρ is larger than unity, interactions between carriers become attractive and favor superconducting correlations at low temperature, while if K_ρ is less than unity, repulsive interactions together with magnetic correlations are enhanced at low temperature.[179]

Furthermore, there exists an added peculiarity in $(TM)_2X$ conductors, since the stoichiometry imposes half a carrier (hole) per TM molecule (and this filling cannot be modified by the applied pressure). Consequently, uniformly spaced molecules along the stacking axis should lead to the situation where the unit cell contains half a carrier; that is, the conduction band is quarter-filled. However, nonuniformity of the molecular packing had been noticed from the early structural studies of $(TMTTF)_2X$ crystals.[97] There exists a dimerization of the overlap between molecules along the stacks: a situation which is more developed in the sulfur series, although it is still encountered in some members of the $(TMTSF)_2X$ series; see Table 1. The impact of the dimerization on the electronic structure is usually quantified by the modulation of the intrastack overlap integral, as both longitudinal and transverse molecular displacements are able to contribute to the modulation of the intermolecular overlap and could contribute to make them half-filled band compounds.

The commensurate band filling opens a new scattering channel for the carriers between both sides of the Fermi surface, as then the total momentum tranfer for two (four) electrons from one side of the 1D Fermi surface to the other is equal to a reciprocal lattice vector (Umklapp scattering for half (quarter)-filled bands).

Commensurability leads to important modifications in the model of the gapless Luttinger liquid, which instead becomes a Mott−Hubbard type insulator with a gap in the charge sector, although, on account of the spin−charge separation of the 1D physics, the spin sector remains gapless.[179] The amplitude of the charge gap relies very strongly on the band filling and the strength of the e−e repulsions of the 1D electronic spectrum. For half-filled band 1D conductors the Mott−Hubbard gap opens up as soon as interactions between carriers are infinitesimally repulsive, namely, $K_\rho < 1$; see Figure 29. Quarter-filled band conductors, however, can afford more repulsive interactions before turning into 1D insula-
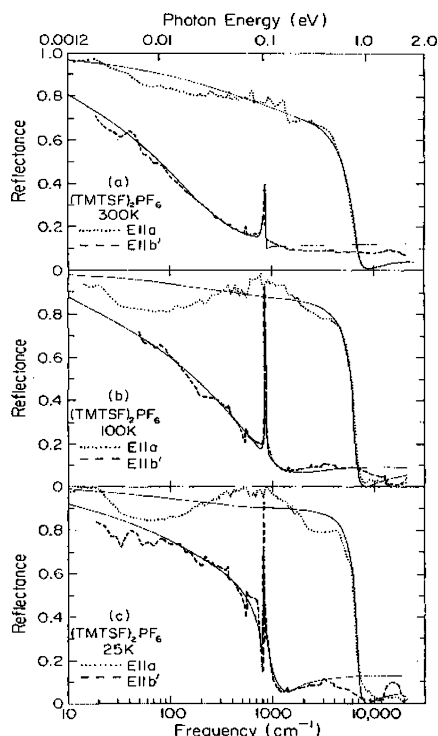
Figure 30. Reflectance data for $(TMTSF)_2PF_6$ at decreasing temperatures from a to c with the light polarized along a or the b' transverse axis. A tranverse plasma edge is observed at low temperature. (Reprinted with permission from ref 181. Copyright 1983 American Physical Society.)

tors. They become insulating when the condition $K_\rho < 0.25$ is fulfillled.

The gap in the density of states at the Fermi energy reads

$$2\Delta_\rho \approx W\left(\frac{g_U}{W}\right)^{1/(2-2n^2K_\rho)} \qquad (8)$$

where g_U is the coupling constant $g_U = W(U/W)^3$ and $n = 2$ (1) for the quarter (half)-filled situation, respectively, in the Hubbard limit.

4.7. 1D Physics High Temperature Regime

The first important question to be settled is whether there exists a part of the generic $(TM)_2X$ diagram where 1D physics is relevant, and the second is where is this region located. According to band calculations, the transverse overlap $t_\perp$ along the b direction is of order 120 and 200 K for sulfur and selenium compounds, respectively.[100] Therefore, it is quite natural to expect 1D theory, first, to govern the physics of these quasi 1D conductors, at least in the high temperature regime when $T > t_\perp$,[126] and, second, to observe a crossover toward higher dimensionality physics below room temperature.

As observed very early in the polarized reflectance studies of $(TMTSF)_2PF_6$ (Figure 30), a plasma edge for the light polarized along the a-axis is observed around 7000 cm^{-1} already at 300 K and becomes even sharper at lower temperatures. However, a transverse plasma edge along the b-axis becomes observable in the vicinity of 1000 cm^{-1} only below 100 K[180,181] and therefore suppresses the revelance of 1D
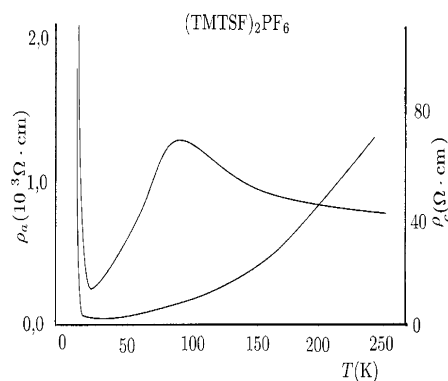
Figure 31. $(TMTSF)_2PF_6$: temperature dependence of the parallel and transverse (c-axis) resistivity. (Reprinted with permission from ref 184. Copyright 1998 EDP Sciences.)

physics restricted to the high temperature limit. The situation is more delicate for $(TMTTF)_2PF_6$, which is already a semiconductor from 300 K according to the frequency dependence of the conductivity showing a peak of oscillator strength around 2000 cm^{-1} at room temperature.[182] More recent optical investigations performed on the same compound at low temperature[183] concluded the existence of a gap in the single particle spectrum of order 800 cm^{-1}. In the following we shall see that this insulating character is indeed a direct consequence of strong electron−electron repulsions and one-dimensionality.

4.7.1. Longitudinal versus Transverse Transport

Studies of the dc transport have provided important clues regarding the domain of 1D physics. The striking behavior of the transport properties emerges from a comparison between the temperature dependence of longitudinal and transverse components of the resistivity (Figure 31).[184] In particular, a lot can be learned about the physics of the $a−b$ layers from the temperature dependence of the transverse transport even (especially) when this latter is incoherent between the layers.

From the early measurements in $(TMTSF)_2PF_6$, opposite temperature dependences for ρ_a and ρ_c had been reported in the high temperature regime.[180] This phenomenon was revisited later, including high pressure studies on $(TMTSF)_2PF_6$ and $(TMTTF)_2PF_6$[184] and, recently, on the extensive high pressure investigation of $(TMTTF)_2PF_6$.[109]

The behavior of the resistance along the direction of weakest coupling, that is, along the c-axis, displays an insulating character with a maximum around 120 K and becomes metallic at lower temperatures, although remaining several orders of magnitude above the Mott−Ioffe critical value which marks the limit between metal-like and insulating-like transport (Figure 31).[185] The insulating character of the transverse transport has been interpreted as the signature of non-Fermi−Landau behavior for the carriers within the planes (chains). When the transverse transport along the c direction is incoherent, the transverse conductivity probes the physics of the ab planes, and the conductivity in terms of the
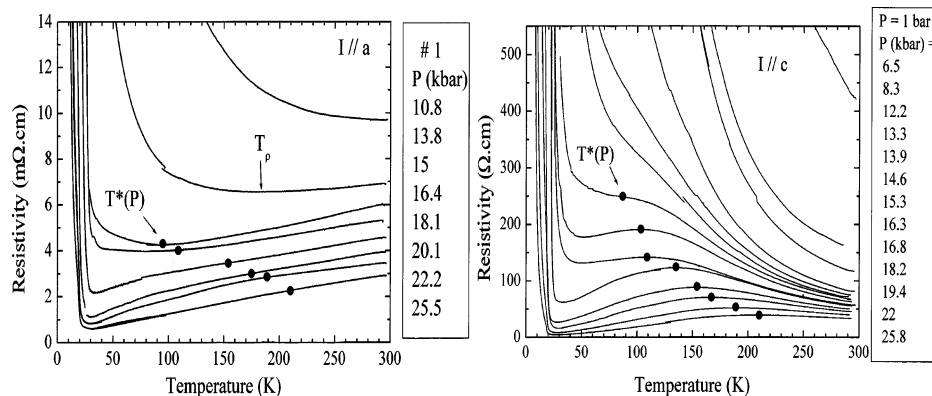
Figure 32. (TMTTF)$_2$PF$_6$ longitudinal (left) and transverse (right) resistance versus temperature at different pressures. (Reprinted with permission from ref 109. Copyright 2004 EDP Sciences.)

transverse coupling $t_\perp$ reads in the tunneling approximation

$$\sigma_\perp(\omega,T) \alpha t_\perp^2 \int dx \int d\omega' \, A_{1D}(x,\omega') \times$$

$$A_{1D}(x,\omega+\omega') \frac{f(\omega') - f(\omega'+\omega)}{\omega} \quad (9)$$

where $A_{1D}(x,\omega)$ is the one-electron spectral function of a single chain. When the ab plane is an array of weakly interacting Luttinger chains, eq 9 leads to a power law temperature dependence for the c-axis conduction.

In the case of a Landau−Fermi electron gas in which electron states are characterized by an in-chain (or in-plane) lifetime τ, the previous equation recovers the proportionality between $\sigma_\perp$ and $\sigma_\parallel$ which had been established at the time of TTF−TCNQ using the Fermi golden rule for incoherent transverse transport.[58] The temperature at which the c axix transport changes from insulating to metallic temperature dependence corresponds to a crossover between two regimes: a high temperature regime with no quasi particle (QP) weight at Fermi energy (possibly a TL liquid in the 1D case) and another regime in which QP weight grows going to low temperature. This interpretation does not necessarily imply that the transport along the c direction must also become coherent below the crossover. The c-axis transport may well remain incoherent with a Fermi liquid establishing in the ab plane with the temperature decreasing below T^*. In the case of (TMTSF)$_2$-PF$_6$, it has been noticed that the Hall voltage which involves the conduction in the ab plane displays a marked minimum[186] at the same T^* where the c-axis resistivity goes through a maximum.[184] However, other Hall measurements performed in a different geometry[187] failed to reproduce the minimum of Hall voltage mentioned in ref 186. Some data of Hall conductivity performed in (TMTSF)$_2$ReO$_4$[188] have provided results in agreement with the data in ref 186 given the limited accuracy of the measurements in ref 188 and the fact that the crossover temperature for (TMTSF)$_2$ReO$_4$ at ambient pressure is located below the anion ordering temperature.[189] Since the theory of the Hall effect for coupled TL chains is not yet very much advanced, we cannot tell more about the interpetation of the Hall voltage.[190,191]

The existence of opposite temperature dependences between transverse and in-chain transport is not restricted to organic conductors and even to 1D conductors, as this property has been observed in a large number of anisotropic conductors. Some examples are given by underdoped high T_c cuprates[192] and layered conductors, (Bi)$_{0.5}$(Pb$_{0.5}$)$_2$Ba$_3$Co$_2$O$_y$ and NaCo$_2$O$_4$,[193] or the quasi 1D cuprate PrBa$_2$Cu$_4$O$_8$.[194]

The transverse conduction derived from eq 9 is also related to the weight of QPs at the Fermi energy. Angle resolved photoemission studies (ARPES) in inorganic low dimensional systems have actually confirmed the existence of a correlation between the insulating character of $\rho_\perp$ and the absence of quasi particle peaks in the above-mentioned layered materials.[193] Furthermore, the emergence of a quasi particle peak in ARPES at low temperature in those inorganic 2D conductors correlates with the transverse transport becoming metal-like.

4.7.2. (TMTTF)$_2$PF$_6$ Phase Diagram

The study of the strongly insulating system (TMTTF)$_2$PF$_6$ under high pressure has been very rewarding not only because it enabled the stabilization of superconductivity in a sulfur compound but also because its location at the left end of the (TM)$_2$X diagram allows several key properties of quasi 1D conductors to be studied under pressure: longitudinal versus transverse transport and one-dimensional deconfinement.[109] The phase diagram in Figure 33 was obtained with (TMTTF)$_2$PF$_6$ taken as the reference compound from the pressure dependence of ρ_c-(T) and $\rho_a(T)$. In the low pressure region (P < 10 kbar), both $\rho_c(T)$ and $\rho_a(T)$ are activated, although an important difference is noticed between activation energies, $\Delta_a < \Delta_c$. Moving toward higher pressures, the activation of ρ_c persists with a gentle decrease of Δ_c under pressure while Δ_a collapses at a pressure of ≈14 kbar, which also marks the onset of the crossover temperature T^*, as shown by the T dependence of ρ_c. The different values and pressure dependences of the activation energies have been taken as an evidence for an in-chain conduction provided by thermally excited 1D objects similar to the solitons in conducting polymers[195] whereas transverse transport requires the excitation of quasi particles through a Mott−Hubbard gap larger than the soliton gap. More recent studies performed in other compounds
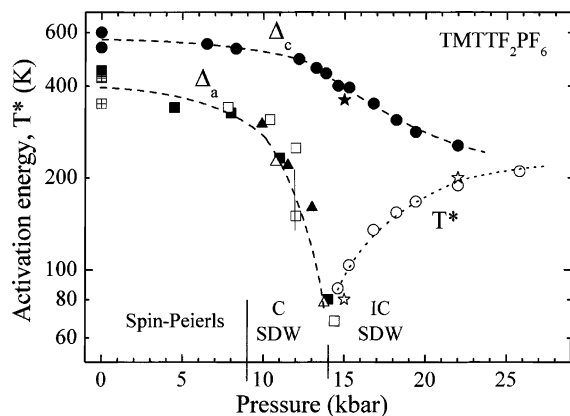
Figure 33. $(TMTTF)_2PF_6$ temperature−pressure phase diagram derived from parallel and transverse transport. The activation for the c-axis transport (Δ_c), although decreasing, survives up to high pressure, while the longitudinal transport (Δ_a) is no longer activated above 15 kbar when a dimensional crossover occurs at finite temperature. The stars (closed and open) at 15 kbar represent the values of Δ_c and T^* measured for the compound $(TMTSF)_2PF_6$ at ambient pressure while the open star at 21 kbar is the value of T^* under 9 kbar. (Reprinted with permission from ref 109. Copyright 2004 EDP Sciences.)

of the $(TMTTF)_2X$ series with X = ReO_4, BF_4, and Br have shown that the main features observed in $(TMTTF)_2PF_6$ under pressure are also observed in the other systems; in particular, the signature of the crossover is recovered and does not depend on the symmetry of the anion.[196]

4.7.3. Dimensionality Crossover under Pressure

The temperature T^* corresponding to the c-resistance maximum moves up under pressure and reaches room temperature under 10 kbar. This temperature can be attributed to the beginning of a crossover between 1D and 2D regimes. The strong pressure dependence of the crossover temperature T^* is a remarkable phenomenon of the TM_2X physics. According to the pressure data of ρ_c for different compounds belonging to the $(TM)_2X$ series, the pressure dependence of T^* is about 10 times larger than that of $t_\perp$ (which is typically 2% kbar^{-1}). This feature suggests that T^* is actually a renormalized version of the bare temperature $t_\perp$ due to the 1D confinement via intrastack electron−hole interactions.[197] As far as insulating $(TMTTF)_2X$ compounds are concerned, the crossover is meaningless, as the strong one-dimensionality renormalization makes T^* irrelevant[197] and transport remains 1D down to the lowest temperature.

4.8. (TM)₂X Compounds: Half- or Quarter-Filled Band Conductors?

When the density of states is gapped ($2\Delta_\rho$) by correlation effects, then the longitudinal transport is expected to vary according to a power law,

$$\rho_{\parallel} \approx T^{4n^2K_\rho - 3} \tag{10}$$

in the high temperature regime, that is, $T > \Delta_\rho$.[179] The material looks like a metal, although this may be true only for the parrallel direction, with a
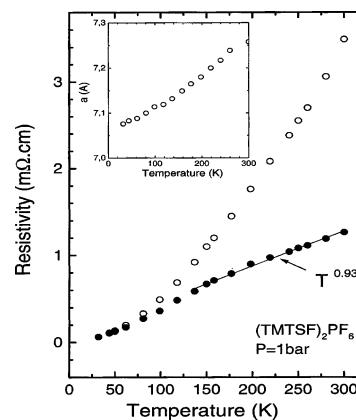
Figure 34. Temperature dependence of the $(TMTSF)_2PF_6$ longitudinal resistance at constant volume showing a quasi linear T dependence, with the thermal dependence of the a parameter displayed in the inset. (Reprinted with permission from ref 198. Copyright 1999 World Scientific.)

transport along the c direction remaining incoherent, showing an insulating dependence in the same temperature domain probing the density of quasi particle states in the ab planes following eq 9.

In the high T regime, the picture of noncoupled chains is approached. Therefore, the density of quasi particle states should resemble the situation which prevails in a Luttinger liquid, namely, $N(E) \approx |\omega|^\alpha$, where α is related to K_ρ by $\alpha = \frac{1}{4}(K_\rho + 1/K_\rho - 2)$, neglecting the influence of the Mott gap, which is small compared to the temperature. Experimentally, the longitudinal resistivity of $(TMTSF)_2PF_6$ is metal-like down to the SDW transition at 12 K, varying sublinearly ($\approx T^{0.93}$) from 300 to 150 K once the constant volume correction is taken into account and more like T^2 below 150 K;[198] see Figure 34.

The experimental power law of the longitudinal resistivity leads in turn to $n^2K_\rho = 0.98$ according to eq 10.

Another approach to the correlation coefficient is provided by optical studies. The study of the far-infrared (FIR) conduction of $(TMTSF)_2PF_6$ (Figure 35) has been very helpful for the determination of K_ρ, since the far-IR gap of about $\Delta_\rho = 200 \text{ cm}^{-1}$ in $(TMTSF)_2PF_6$ has been attributed to the signature of the Mott−Hubbard gap.[199] The theory predicts a power law dependence for the optical conductivity at frequencies larger than the Mott gap,[179] namely,

$$\sigma(\omega) \approx \omega^{4n^2K_\rho - 5} \tag{11}$$

at $\omega > 2\Delta_\rho$. According to the optical experimental data,[199] $\sigma(\omega) \approx \omega^{-1.3}$ at high frequency, and thus, a value of $n^2K_\rho = 0.93$ is obtained. This value for the correlation coefficient is fairly close to the one derived from parrallel transport data, but none of these experiments allow us to discriminate between half- or quarter-filled Umklapp scattering.

In the early days of the $(TM)_2X$ compounds, the lattice dimerization was believed to govern the amplitude of the Mott−Hubbard gap.[200,201] However, later, an alternative interpretation based on new experimental results was proposed, assuming that the quarter-filled scattering could justify the existence of the Mott gap in the whole $(TM)_2X$ series.[179]
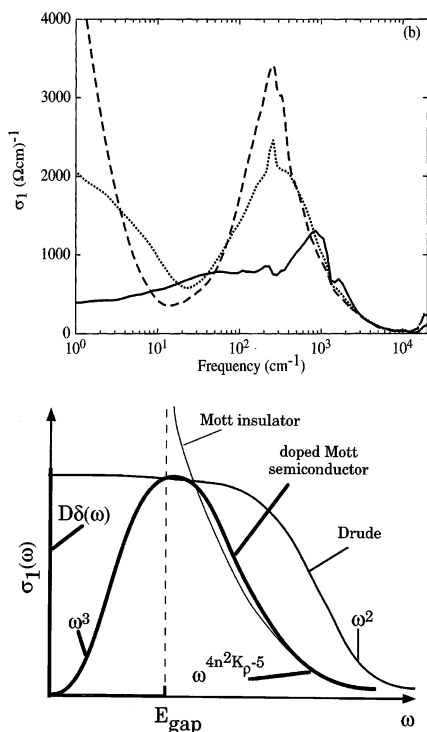
Figure 35. Far-infrared data of $(TMTSF)_2PF_6$: experiment (top) (Reprinted with permission from ref 199. Copyright 1998 American Physical Society.) and theory (bottom) (Reprinted with permission from ref 179. Copyright 1997 Elsevier.).

If we choose the half-filled hypothesis ($n = 1$), thus, K_ρ is close to unity, implying that the system is weakly coupled. This situation of very weak coupling is hard to reconcile with the enhancement of the spin susceptibility,[100] but an additional argument against weak coupling is given by the unusual behavior of the transverse transport.

As far as the transverse transport is concerned, a temperature dependence such as $\rho_c(T) \approx T^{1-2\alpha}$ can be anticipated in the 1D regime $(T > T^*)$[202] if the density of states of a Luttinger liquid is governing the density of excited quasi particles at high temperature. The weak coupling value for K_ρ derived from the temperature dependence of the longitudinal transport and the optical data would imply $\alpha \approx 0$ and consequently a metal-like temperature dependence for $\rho_c(T)$ which is *at variance* with the data.

If we take now the quarter-filled hypothesis $n = 2$, then the fit of the experimental data would lead to $K_\rho = 0.23$ and $\alpha = 0.64$.[199] This value for K_ρ agrees fairly well with the quarter-filled scenario and $W = 12\,000$ K (from band structure calculations and plasma edge measurements), $\Delta_\rho = 200$ cm^{-1} (from far-IR data), and $U/W = 0.7$ (which is in fair agreement with the enhancement of the spin susceptibility at low temperature).[100] Such a strong coupling value for K_ρ implies that a system such as $(TMTSF)_2PF_6$ lies at the border between a 1D Mott insulator and a Luttinger liquid, though slightly on the insulating side.

Since studies of parallel and transverse transport have been carried on in $(TMTTF)_2PF_6$ under pressure, this latter compound provides the possibility to study the gentle evolution from Mott insulation

to Luttinger liquid induced by pressure. Turning to the evaluation of the correlation coefficient from the temperature dependence of ρ_c and the law $\rho_c(T) \approx T^{1-2\alpha}$, which is expected to hold in the regime of uncoupled Luttinger chains, we end up fitting the data for $(TMTTF)_2PF_6$ in the pressure domain around 12 kbar (Figure 33) with very small values of K_ρ (large values of α), which are not compatible with the value $K_\rho = 0.23$ derived from far-IR and NMR data.[100] Consequently, we are forced to accept that the preexistence of a Mott gap cannot be forgotten and that the excitation of a single particle through the remnant of the Mott gap of the order of 220 K in $(TMTSF)_2PF_6$ is still the dominant factor for the temperature dependence of the transverse transport along c[202] with a transverse resistivity behaving as $\rho_c(T) \propto T^{1-2\alpha} \exp \Delta_\rho/T$. The neglect of the Mott gap may become a valid approximation at higher pressures.

Since the Mott−Hubbard gap varies exponentially with K_ρ, even a small variation of the ratio between the Coulomb interaction and the bandwidth under pressure can explain a large decrease of $2\Delta_\rho$ moving from the left to the right in the generic phase diagram. Both optical and transport data give $2\Delta_\rho = 800-1000$ K in $(TMTTF)_2PF_6$ at ambient pressure.[109] The difference between K_ρ for selenium and sulfur compounds ($K_\rho = 0.18$ for the latter material) can be afforded by the difference of their bare bandwidths, as the on-site repulsion, being a molecular property, is likely to be less sensitive to pressure than the intermolecular overlap along the stacking axis. The lesson from this section is that all members in the phase diagram $(TM)_2X$ are indeed 1D confined Mott insulators with a correlation gap evolving rapidly under pressure due to the pressure induced band broadening. $(TMTSF)_2PF_6$ under ambient pressure looks like a 1D metal at high temperature because the temperature is large compared to the Mott gap. This compound remains a metal below the crossover temperature T^* only because one-dimensional carriers become deconfined by a transverse coupling which becomes then larger than the Mott gap.[179]

4.9. Pseudogap and Zero Frequency Mode

It is also most illuminating to have a look at the conductivity in the far-infrared regime. A large gap of order 1000 K is observed in the frequency dependence of the far-IR conductivity of sulfur compounds.[182] This is in line with the activation energy of the dc conductivity in those compounds. However, the surprise arose for selenium compounds, which behave apparently like normal metals as far as dc tranport is concerned, despite the marked gap observed in the far-IR regime at low temperature (Figure 36). The apparent normal behavior of the resistivity varying quadratically in temperature for $(TMTSF)_2ClO_4$ or $(TMTSF)_2PF_6$ above the SDW transition could lead to the misleading conclusion of a 2- or 3D Fermi gas in which the temperature dependence of the transport is governed by e−e scattering. However, the analysis of the conductivity in terms of the frequency reveals quite a striking breakdown of the Drude theory for single particles. The inability
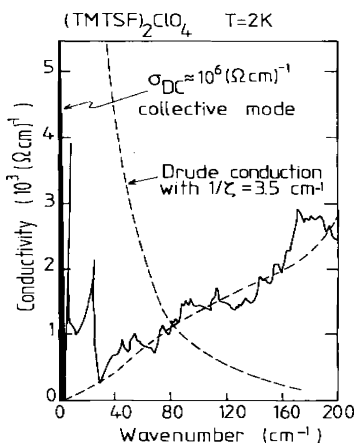
Figure 36. Far-infrared data of $(TMTSF)_2ClO_4$ from ref 206. The dashed line is the Drude behavior with $1/\tau = 3.5$ cm^{-1} and $\omega_p = 10^4$ cm^{-1}. (Reprinted with permission from ref 206. Copyright 1983 EDP Sciences.)

of the Drude theory to describe the optical conductivity has been noticed by a number of experimentalists working on $(TMTSF)_2X$ with $X = ClO_4$, PF_6, or SbF_6.[203] When the reflectance of $(TMTSF)_2ClO_4$ in the near-infrared is analyzed with the Drude model in the whole range of temperatures from 300 down to 30 K, the electron scattering rate is found to decrease gradually from 2.5×10^{14} s^{-1} at room temperature (RT) to 1.3×10^{14} s^{-1} at 30 K.[204] Even if the RT value is not far from the value from dc conductivity, a drastic difference emerges at low temperature, as σ_{dc} increases by a factor about 100 between RT and 30 K,[93] as compared to the factor 2 for the optical lifetime.

Another striking feature of the optical conductivity has been noticed when the Kramers–Krönig (K–K) transformation of the reflectance is performed in a broad frequency domain for $(TMTSF)_2ClO_4$ as well as for all conducting materials at low temperature. Given the usual Drude relation $\sigma_{dc} = \omega_p^2\tau/4\pi$ between transport lifetime and plasma frequency data (the plasma frequency has been found to be nearly temperature independent[204,181]) and the measured resistance ratio for ρ_a of about 800 between RT and 2 K obtained in good quality measurements, the Drude conductivity in the frequency range $\approx$40 cm^{-1} should amount to at least 4000 $(\Omega$ cm$)^{-1}$.[205,206] The measured optical conductivity is at most of the order of 500 $(\Omega$ cm$)^{-1}$.[205] Consequently, the rise in the conductivity as $\omega \rightarrow 0$ has been taken, in $(TMTSF)_2ClO_4$ as well as in the other salts with PF_6 or SbF_6, as an evidence for a hidden zero frequency mode. This mode is actually so narrow that it escapes a direct determination from K–K analysis of the reflectance, which is limited to the frequency domain above 10 cm^{-1}. Estimates of the mode width have been obtained using the dc conductivity and the oscillator strength Ω_p^2 of the mode with $\sigma_{dc} = \Omega_p^2\tau_c/4\pi$, where Ω_p is measured from the first zero crossing of the dielectric constant. This procedure gives a damping factor $\Gamma_c = 0.005$ and 0.09 cm^{-1} at 2 and 25 K, respectively, in $(TMTSF)_2ClO_4$.[206] The confirmation of a very long scattering time for the dc conduction has also been brought by the rapid suppression of T_c by nonmagnetic defects in the nonconventional superconductor

$(TMTSF)_2ClO_4$, leading to $\Gamma_c = 0.13$ cm^{-1} at low temperature,[147] meaning that the elctron lifetime at low temperature is actually much longer than the value inferred from a Drude description.

There is now a wealth of experimental evidences showing the development of a narrow frequency mode in the Mott gap of $(TMTSF)_2ClO_4$ and related conducting compounds. From far-IR data in $(TMTSF)_2PF_6$, it has also been shown that the narrow mode carries only a small fraction (a few percent) of the total spectral weight[199,181] but it is this mode which explains the very large value of the dc conduction observed at low temperature.[99]

5. Summary

Discovering new materials with the highest possible $T_{c,s}$ has always been a large objective of condensed matter research. Such a motivation applies, in particular, to the field of organic conductors, which bloomed in the early 1970s after the announcements on TTF–TCNQ claiming the possibility of superconducting phenomena at provocative temperatures. Superconductivity became reality only five years later with the discovery of $(TMTSF)_2PF_6$. However, charge-transfer (TTF–TCNQ, TSeF–TCNQ, or TM–DM) and molecular salts [$(TM)_2X$] are the only two series surveyed in this short article, since they can be considered as the prototype systems in which most of the experimental results have be obtained.

The study of TTF–TCNQ has emphasized the role of several parameters, such as one-dimensional electronic structure, intrachain (interchain) Coulomb and electron–phonon coupling, incommensurability, and commensurability. Depending on the relative strength of these parameters, a wealth of behaviors can be obtained. One-dimensionality is the key parameter behind most porperties of TTF–TCNQ. There is also considerable evidence for strong intrachain Coulomb interactions in this conductor from the enhanced susceptibility, the NMR relaxation time data, and the observation of $4k_F$ diffuse scattering coming from the TTF stacks. Furthermore, from NMR results it seems that Coulomb interactions are also important on the TCNQ stacks, and within the 1D Hubbard model $U/t_\parallel \approx 1$–1.5. Transverse overlap is small in TTF–TCNQ as compared to the dominant transverse Coulomb interaction which is responsible for the 3D ordering of the CDW fluctuations in an insulating Peierls state at 54 K. SDW fluctuations are also diverging in the 1D model but do not order because of the smallness of the interchain overlap of these compounds. Electron–phonon coupling is important, as shown by the phonon softening at $2k_F$ and the fluctuations of the CDW on the TCNQ stacks at high temperature, which contribute to most of the conduction in the metallic regime outside the commensurability domain under pressure. The failure of TTF–TCNQ to develop superconductivity can be explained by the initial small value of the interchain overlap (overcome by the Coulomb coupling) and the robustness of the Peierls state under pressure.

$(TM)_2X$ single chain compounds are different from TTF–TCNQ in several respects. The interchain overlap is considerably larger (about a factor 10 or

so), and the band filling is commensurate, as determined by the chemistry, and, in turn, independent of the applied pressure.

To summarize, the picture emerging for the TM_2X phase diagram is that of a Mott insulating phase with a correlation gap decreasing from sulfur to selenium compounds (Figure 21). Optical and transport data under pressure make the quarter-filled Umklapp scattering a likely mechanism for the existence of the Mott gap. This hypothesis is actually corroborated by the observation of a large Mott gap in a quarter-filled compound lacking the half-filled Umklapp scattering for symmetry reasons.[207] As long as the Mott gap is large (say more than 300 K), the 1D confinement is quite active and the single particle interstack hopping remains meaningless, despite a bare value of the transverse coupling, still of the order of 100 K. Moving toward the right in the generic phase diagram, the decrease of the Mott gap (because of the bandwidth increasing under pressure at a rate of about $1-2\%$ kbar^{-1}) makes the renormalization of the transverse hopping less pronounced. $(TMTSF)_2PF_6$ is a compound in which the dimensional crossovers at T^* and $2\Delta_\rho$ are both of the same order of magnitude ($\approx 150-200$ K). T^* is further increased under pressure in $(TMTSF)_2PF_6$ or chemically, as for $(TMTSF)_2ClO_4$, where it reaches room temperature under ambient pressure, according to the data of ρ_c,.[208] Below T^* the system becomes an anisotropic conductor: first a two-dimensional conductor with high energy excitations governed by the Mott gap and ultimately an anisotropic three-dimensional Fermi liquid around 5 K (for $(TMTSF)_2$-ClO_4 under ambient pressure).

The nature of the superconducting coupling is not yet settled, although its great sensitivity to nonmagnetic disorder and the observation of critical fields overcoming the Pauli limit point toward non-s wave coupling.

The existence of a very narrow mode which accounts for the large value of the dc conductivity together with a pseudogap in the far-infrared regime of the single particle spectrum is a common feature of the metallic regime in both systems, that is, just above the Peierls transition in TTF−TCNQ or in the low temperature metallic regime of $(TMTSF)_2X$ compounds. In both cases, the collective mode carries only a minor fraction of the total spectral weight.

This article was mainly focused on the high temperature properties of the prototype 1D organic conductors. A lot of interesting results have also been obtained in the ground states of these compounds, including the discovery of new phenomena, such as the magnetic field induced spin density wave phases and magnetoangular oscillations in $(TMTSF)_2X$.[121,209] The reader interested in further references could consult the following textbooks and recent conference proceedings.[127,175,210−216] It is also clear that a lot of fascinating questions are still open, waiting for unambiguous experimental evidences. The actual symmetry of the order parameter (triplet or singlet) is definitely one of them.

7. References

(1) Onnes, H. *Proc. Akad. Wetenshaffen* **1911**, *14*, 113.
(2) Bednorz, J.; Müller, K. *Z. Phys. B* **1986**, *64*, 189.
(3) London, F. *J. Chem. Phys.* **1937**, *5*, 837.
(4) McCoy, H.; Moore, W. *J. Am. Chem. Soc.* **1911**, *33*, 273.
(5) Akamatsu, H.; Inokuchi, H.; Matsunaga, Y. *Nature* **1954**, *173*, 168.
(6) Little, W. *Phys. Rev. A* **1964**, *134*, 1416.
(7) Little, W. *Sci. Am.* **1965**, *212*, 21.
(8) Bardeen, J.; Cooper, L.; Schrieffer, J. *Phys. Rev.* **1957**, *108*, 1175.
(9) Ginzburg, V. *J. Polym. Sci. C* **1970**, *29*, 3.
(10) Little, W. *J. Polym. Sci. C* **1970**, *29*, 17.
(11) André, J.; Bieber, A.; Gautier, F. *Ann. Phys.* **1976**, *I*, 145.
(12) Shchegolev, I. *Phys. Status Solidi A* **1972**, *12*, 9.
(13) Burarov, L.; Fedutin, D.; Shchegolev, I. *Zh. Eksp. Teor. Fiz.* **1970**, *59*, 1125.
(14) Epstein, A.; Etemad, S.; Garito, A.; Heeger, A. *Phys. Rev. B* **1972**, *5*, 952.
(15) Pouget, J.; Comès, R.; Epstein, A.; Miller, J. *Phys. Rev. B* **1980**, *21*, 486.
(16) Pouget, J.; Comès, R.; Epstein, A.; Miller, J. *Mol. Cryst. Liq. Cryst.* **1982**, *85*, 203.
(17) Wudl, F.; Smith, G.; Hufnagel, E. *J. Chem. Soc., Chem. Commun.* **1970**, 1453.
(18) Ferraris, J.; Cowan, D.; Walatka, W.; Perlstein, J. *J. Am. Chem. Soc.* **1973**, *95*, 948.
(19) Garito, A.; Heeger, A. *Acc. Chem. Res.* **1974**, 7, 232.
(20) Berlinsky, A.; Carolan, J.; Weiler, L. *Solid State Commun.* **1974**, *15*, 795.
(21) Coleman, L. *Solid State Commun.* **1973**, *12*, 1125.
(22) Hulm, J.; Matthias, B. *Science* **1980**, *208*, 881.
(23) Peierls, R. *Quantum Theory of Solids*; Oxford University Press: London, 1955.
(24) Thomas, G. *Phys. Rev. B* **1978**, *13*, 5105.
(25) Jérome, D.; Schulz, H. *Adv. Phys.* **1982**, *31*, 299.
(26) Friend, R. H.; Miljak, M.; Jérome, D. *Phys. Rev. Lett.* **1978**, *40*, 1048.
(27) Takahashi, T.; Jérome, D.; Masin, F.; Fabre, J.; Giral, L. *J. Phys. C: Solid State Phys.* **1984**, *17*, 3777.
(28) Jérome, D.; Müller, W.; Weger, M. *J. Phys. Lett.* **1974**, *35*, L-77.
(29) Tomkiewicz, Y.; Taranko, A.; Torrance, J. *Phys. Rev. Lett.* **1976**, *36*, 751.
(30) Denoyer, F.; Comès, R.; Garito, A.; Heeger, A. *Phys. Rev. Lett.* **1975**, *35*, 445.
(31) Kagoshima, S.; Anzai, H.; Kajimura, K.; Ishiguro, T. *J. Phys. Soc. Jpn.* **1975**, *39*, 1143.
(32) Comés, R.; Shapiro, S.; Shirane, G.; Garito, A.; Heeger, A. *Phys. Rev. Lett.* **1975**, *35*, 1518.
(33) Wang, Z.; Girard, J.; Pasquier, C.; Jérome, D.; Bechgaard, K. *Phys. Rev. B* **2003**, *67*, R-121401.
(34) Abrahams, E.; Solyom, J.; Woynarovich, F. *J. Phys., Colloq.* **1977**, *38*, C7-254.
(35) Barisić, S.; Bjeliś, A. *J. Phys., Colloq.* **1977**, *38*, C7−254.
(36) Bjeliś, A.; Barisić, S. *Phys. Rev. Lett.* **1976**, *33*, 1517.
(37) Kagoshima, S.; Ishiguro, T.; Anzai, H. *J. Phys. Soc. Jpn.* **1976**, *41*, 2061.
(38) Bouveret, Y.; Megtert, S. *J. Phys. (Paris)* **1989**, *50*, 1649.
(39) Fröhlich, H. *Proc. R. Soc. London, A* **1954**, *223*, 296.
(40) Bardeen, J. *Solid State Commun.* **1973**, *13*, 357.
(41) Allender, D.; Bray, J.; Bardeen, J. *Phys. Rev. B* **1974**, *9*, 119.
(42) Grüner, G.; Monceau, P. In *Charge Density Waves in Solids*; Gorkov, L. V., Grüner, G., Eds.; North-Holland: Amsterdam, 1989; p 137.

(43) Lee, P.; Rice, T.; Anderson, P. *Solid State Commun.* **1974**, *14*, 703.
(44) Forro, L.; Lacoe, R.; Bouffard, S.; Jérome, D. *Phys. Rev. B* **1987**, *35*, 5884.
(45) Lacoe, R.; Schulz, H.; Jérome, D.; Bechgaard, K.; Johannsen, I. *Phys. Rev. Lett.* **1985**, *55*, 2351.
(46) Fukuyama, H.; Lee, P. *Phys. Rev. B* **1978**, *17*, 535.
(47) Tomić, S.; Fontaine, F.; Jérome, D. *Phys. Rev. B* **1988**, *37*, 8468.
(48) Pouget, J. In *Semiconductors and Semimetals*; Conwell, E.; Ed.; Academic Press: New York, 1988; Vol. 27.
(49) Jérome, D.; Mazaud, A.; Ribault, M.; Bechgaard, K. *J. Phys., Lett.* **1980**, *41*, L95.
(50) Horovitz, B.; Gutfreund, H.; Weger, M. *Phys. Rev. B* **1975**, *12*, 3174.
(51) Chu, C.; Harper, J.; Geballe, T.; Greene, R. *Phys. Rev.* **1973**, *31*, 1491.
(52) Megtert, S.; Comès, R.; Vettier, C.; Pynn, R.; Garito, A. *Solid State Commun.* **1981**, *37*, 875.
(53) McMillan, W. *Phys. Rev. B* **1975**, *12*, 1187.
(54) Herman, F. *Phys. Scr.* **1977**, *16*, 303.
(55) Welber, B.; Seiden, P.; Grant, P. *Phys. Rev. B* **1978**, *118*, 2692.
(56) Jérome, D.; Schulz, H. In *Extended Linear Chain Compounds*; Miller, J. S., Ed.; Plenum Press: New York, 1982; Vol. 2.
(57) Soda, G.; Jérome, D.; Weger, M.; Alizon, J.; Gallice, J.; Robert, H.; Fabre, J. M.; Giral, L. *J. Phys. (Paris)* **1977**, *38*, 931.
(58) Weger, M. *J. Phys. (Paris)* **1978**, *39*, C6-1456.
(59) Voit, J.; Schulz, H. *Phys. Rev. B* **1988**, *37*, 10068.
(60) Basista, H.; Bonn, D.; Timusk, T.; Voit, J.; Jérome, D.; Bechgaard, K. *Phys. Rev. B* **1990**, *42*, 4088.
(61) Bouffard, S.; Chipaux, R.; Jérome, D.; Bechgaard, K. *Solid State Commun.* **1981**, *37*, 405.
(62) Grant, P.; Greene, R.; Wrighton, G.; Castro, G. *Phys. Rev. Lett.* **1973**, *31*, 1311.
(63) Bright, A.; Garito, A.; Heeger, A. *Phys. Rev. B* **1974**, *10*, 1328.
(64) Tanner, D.; Cummings, K.; Jacobsen, C. *Phys. Rev. Lett.* **1981**, *47*, 597.
(65) Eldridge, J.; Bates, G. *Mol. Cryst. Liq. Cryst.* **1985**, *119*, 183.
(66) Gorshunov, B.; Kozlov, G.; Volkov, A.; Zelezny, V.; Petzelt, J.; Jacobsen, C. *Solid State Commun.* **1986**, *60*, 681.
(67) Tanner, D.; Jacobsen, C. *Mol. Cryst. Liq. Cryst.* **1982**, *85*, 137.
(68) Engler, E.; Scott, B.; Etemad, S.; Penney, T.; Patel, V. *J. Am. Chem. Soc.* **1977**, *99*, 5909.
(69) Pouget, J.; Megtert, S.; Comès, R. *Lect. Notes Phys.* **1979**, *95*, 14.
(70) Kagoshima, S.; Ishiguro, T.; Schultz, T.; Tomkiewicz, Y. *Lect. Notes Phys.* **1979**, *95*, 28.
(71) Megtert, S.; Pouget, J.; Comès, R. In *Molecular Metals*; Hatfield, W. E., Ed.; Plenum Press: New York, 1979.
(72) Thomas, J.; Jérome, D. *Solid State Commun.* **1980**, *36*, 813.
(73) Thomas, J. *Solid State Commun.* **1982**, *42*, 587.
(74) Greene, R.; Mayerle, J.; Schumaker, R.; Castro, G.; Chaikin, P.; Etemad, S.; Placa, S. L. *Solid State Commun.* **1976**, *20*, 943.
(75) Bloch, A.; Cowan, D.; Bechgaard, K.; Pyle, R. E.; Banks, R.; Poehler, T. *Phys. Rev. Lett.* **1975**, *34*, 1561.
(76) Korin, B.; Cooper, J.; Miljak, M.; Hamzic, A.; Bechgaard, K. *Chem. Scr.* **1981**, *17*, 45.
(77) Miljak, M.; Andrieux, A.; Friend, R.; Malfait, G.; Jérome, D.; Bechgaard, K. *Solid State Commun.* **1978**, *26*, 969.
(78) Cooper, R.; Weger, M.; Jérome, D.; Lefur, D.; Bechgaard, K.; Bloch, A.; Cowan, D. *Solid State Commun.* **1976**, *19*, 749.
(79) Andersen, J.; Bachgaard, K.; Jacobsen, C.; Rindorf, G.; Soling, H.; Thorup, N. *Acta Crystallogr., B* **1978**, *34*, 1901.
(80) Jacobsen, C.; Mortensen, K.; Andersen, J.; Bechgaard, K. *Phys. Rev. B* **1978**, *18*, 905.
(81) Tomkiewicz, Y.; Andersen, J.; Taranko, A. *Phys. Rev. B* **1978**, *17*, 1579.
(82) Pouget, J. *Chem. Scr.* **1981**, *55*, 85.
(83) Andrieux, A.; Duroure, C.; Jérome, D.; Bechgaard, K. *J. Phys., Lett.* **1979**, *40*, 381.
(84) Andrieux, A.; Chaikin, P.; Duroure, C.; Jérome, D.; Weyl, C.; Bechgaard, K.; Andersen, J. *J. Phys. (Paris)* **1979**, *40*, 1199.
(85) Andrieux, A.; Bechgaard, K.; Duroure, C.; Jérome, D. *C. R. Acad. Sci.* **1979**, *288*, 351.
(86) Brun, G.; Peytavin, S.; Liautard, B.; Maurin, E. T.; Fabre, J.; Giral, L. *C. R. Acad. Sci. (Paris)* **1977**, *284C*, 211.
(87) Bechgaard, K.; Jacobsen, C.; Mortensen, K.; Pedersen, H.; Thorup, N. *Solid State Commun.* **1979**, *33*, 1119.
(88) Pouget, J. P.; Ravy, S. *Synth. Met.* **1997**, *85*, 1523.
(89) Overhauser, A. *Phys. Rev. Lett.* **1960**, *9*, 462.
(90) Lomer, W. M. *Proc. Phys. Soc.* **1962**, *80*, 489.
(91) Balicas, L.; Behnia, K.; Kang, W.; Canadell, E.; Auban-Senzier, M. R.; Jérome, D.; Fabre, J. *J. Phys. I* **1994**, *4*, 1539.
(92) Parkin, S.; Ribault, M.; Jérome, D.; Bechgaard, K. *J. Phys. C* **1981**, *14*, L-445.
(93) Bechgaard, K.; Carneiro, M.; Olsen, M.; Rasmussen, F. *Phys. Rev. Lett.* **1981**, *46*, 852.
(94) Coulon, C.; Delhaes, P.; Flandrois, S.; Lagnier, R.; Bonjour, E.; Fabre, J. *J. Phys. (Paris)* **1982**, *43*, 1059.
(95) Jérome, D. *Science* **1991**, *252*, 1509.
(96) Friedel, J.; Jérome, D. *Contemp. Phys.* **1982**, *23*, 583.
(97) Ducasse, L.; Abderraba, A.; Hoarau, J.; Pesquer, M.; Gallois, B.; Gaultier, J. *J. Phys. C* **1986**, *39*, 3805.
(98) Behnia, K.; Balicas, L.; Kang, W.; Jérome, D.; Carretta, Y. F.; Berthier, C.; Horvatic, M.; Ségransan, P.; Hubert, L.; Bourbonnais, C. *Phys. Rev. Lett.* **1995**, *74*, 5272.
(99) For more references on the ground states of the insulating compounds, see the articles in ref 217.
(100) Bourbonnais, C.; Jérome, D. In *Advances in Synthetic Metals*; Bernier, P., Lefrant, S., Bidan, G., Eds.; Elsevier: Amsterdam, 1999.
(101) Coulon, C.; Parkin, S.; Laversanne, R. *Phys. Rev. B* **1985**, *31*, 3583.
(102) Javadi, H.; Laversanne, R.; Epstein, A. *Phys. Rev. B* **1988**, *37*, 4280.
(103) Laversanne, R.; Coulon, C.; Gallois, B.; Pouget, J. P.; Moret, R. *J. Phys., Lett.* **1984**, *45*, L393.
(104) Chow, D.; Zamborsky, F.; Alavi, B.; Tantillo, D.; Baur, A.; Merlić, C.; Brown, S. *Phys. Rev. Lett.* **2000**, *85*, 1698.
(105) Zamborsky, F.; Yu, W.; Raas, W.; Brown, S.; Alavic, B.; Merlić, C.; Baur, A.; Lefebvre, S.; Wzietek, P. *J. Phys. IV* **2002**, *12*, Pr-9-139.
(106) Pouget, J. P.; Ravy, S. *J. Phys. I* **1996**, *6*, 1501.
(107) Nad, F.; Monceau, P.; Fabre, J. *J. Phys. IV* **1999**, *9*, Pr-10-361.
(108) Nad, F.; Monceau, P. *J. Phys. IV* **2002**, *12*, Pr-9-133.
(109) Auban-Senzier, P.; Jérome, D.; Carcel, C.; Fabre, J. *J. Phys. IV* **2004**, *114*, 4.
(110) Hirsch, J.; Scalapino, D. *Phys. Rev. B* **1983**, *27*, 7169.
(111) Seo, H.; Fukuyama, H. *J. Phys. Soc. Jpn.* **1997**, *66*, 1249.
(112) Brazovskii, S. *J. Phys. IV* **2002**, *12*, Pr-9.
(113) Seo, H.; Kuwabara, M.; Ogata, M. *J. Phys. IV* **2002**, *12*, Pr-9-205.
(114) Moret, R.; Pouget, J. P.; Comès, R.; Bechgaard, K. *J. Phys. (Paris)* **1985**, *46*, 1521.
(115) Ribault, M.; Jérome, D.; Tuchendler, J.; Weyl, C.; Bechgaard, K. *J. Phys. Lett.* **1983**, *44*, L-953.
(116) Cooper, J.; Kang, W.; Auban, P.; Montambaux, G.; Jérome, D.; Bechgaard, K. *Phys. Rev. Lett.* **1989**, *65*, 1984.
(117) Kang, W.; Cooper, J.; Jérome, D. *Phys. Rev. B* **1991**, *43*, R-11-467.
(118) Naughton, M. J.; Chamberlin, R. V.; Yan, P. M. C.; Hsu, S.; Chiang, L.; Azbel, M. *Phys. Rev. Lett.* **1995**, *61*, 621.
(119) McKernan, S. K.; Hannahs, S. T.; Scheven, U.; Danner, G. M.; Chaikin, P. M. *Phys. Rev. Lett.* **1995**, *75*, 1630.
(120) Kang, W.; Hannahs, S. T.; Chaikin, P. M. *Phys. Rev. Lett.* **1993**, *70*, 3091.
(121) Lebed, A. G. *J. Phys. I* **1996**, *6*, 1819 and references therein.
(122) Tomić, S.; Cooper, J.; Jérome, D.; Bechgaard, K. *Phys. Rev. Lett.* **1989**, *62*, 462.
(123) Moret, R.; Ravy, S.; Pouget, J. P.; Comés, R.; Bechgaard, K. *Phys. Rev. Lett.* **1986**, *57*, 1915.
(124) Tomić, S.; Jérome, D. *J. Phys.: Condens. Matter Lett.* **1989**, *1*, 4451.
(125) Wudl, F.; Nalewajek, D.; Thorup, J. M.; Extine, N. W. *Science* **1983**, *22*, 415.
(126) Emery, V. J. *J. Phys., Colloq.* **1983**, *44*, C3−977.
(127) Ishiguro, T.; Yamaji, K.; Saito, G. *Organic Superconductors*; Springer: Berlin, 1998.
(128) Wilhelm, H.; Jaccard, D.; Duprat, R.; Bourbonnais, C.; Jérome, D.; Moser, J.; Carcel, C.; Fabre, J. *Eur. Phys. J.* **2001**, *B21*, 175.
(129) Kang, W.; Behnia, K.; Jérome, D.; Balicas, L.; Canadell, E.; Ribault, M.; Fabre, J. *Europhys. Lett.* **1995**, *29*, 635.
(130) Ribault, M.; Benedek, G.; Jérome, D.; Bechgaard, K. *J. Phys., Lett.* **1980**, *41*, L-397.
(131) Andres, K.; Wudl, F.; McWhan, D.; Thomas, G.; Nalewajek, D.; Stevens, A. *Phys. Rev. Lett.* **1980**, *45*, 1449.
(132) Garoche, P.; Brusetti, R.; Bechgaard, K. *Phys. Rev. Lett.* **1982**, *49*, 1346.
(133) Mailly, D.; Ribault, M.; Bechgaard, K. *J. Phys.* **1983**, *44, C3*, 1037.
(134) Gubser, D.; Fuller, W.; Poehler, T.; Stokes, J.; Cowan, D.; Lee, M.; Bloch, A. *Mol. Cryst. Liq. Cryst.* **1982**, *79*, 225.
(135) Pouget, J. In *Low Dimensional Conductors and Superconductors*; Jérome, D., Caron, L. G., Eds.; Plenum Press: New York, 1987.
(136) Brusetti, R.; Garoche, P.; Bechgaard, K. *J. Phys. C: Solid State Phys.* **1983**, *16*, 3535.
(137) Miljak, N.; Cooper, J. R.; Bechgaard, K. *J. Phys., Colloq.* **1983**, *44*, 893.
(138) Greene, R.; Haen, P.; Huang, S.; Engler, E.; Choi, M.; Chaikin, P. *Mol. Cryst. Liq. Cryst.* **1982**, *79*, 183.
(139) Murata, K.; Anzai, H.; Kajimura, K.; Ishiguro, T.; Saito, G. *Mol. Cryst. Liq. Cryst.* **1982**, *79*, 283.
(140) Murata, K.; Tokumoto, M.; Anzai, H.; Kajimura, K.; Ishiguro, T. *Jpn. J. Appl. Phys.* **1987**, *Suppl. 26-3*, 1367.
(141) Gorkov, L.; Jérome, D. *J. Phys. Lett.* **1985**, *46*, L-643.
(142) Lee, I.; Chaikin, P.; Naughton, M. *Phys. Rev. B* **2000**, *62*, R14669.
(143) Oh, J.; Naughton, M. *Phys. Rev. Lett.* **2004**, *92*, 067001.
(144) Schulz, H.; Jérome, D.; Ribault, M.; Mazaud, A.; Bechgaard, K. *J. Phys. Lett.* **1981**, *42*, L-51.

(145) Gallois, B. Ph.D. Thesis, University Bordeaux I, 1987.
(146) Mailly, D. Ph.D. Thesis, Thesis Université d'Orsay, 1983.
(147) Joo, N.; Pasquier, C.; Auban-Senzier, P.; Jérome, D. *Eur. Phys. J. B* **2004**, *40*, 43.
(148) Creuzet, F.; Jérome, D.; Moradpour, A. *Mol. Cryst. Liq. Cryst.* **1985**, *119*, 297.
(149) Murata, K.; Brossard, L.; Lacoe, R.; Ribault, M.; Jérome, D.; Bechgaard, K.; Moradpour, A. *Mol. Cryst. Liq. Cryst.* **1985**, *119*, 245.
(150) Kang, W.; Hannahs, S.; Chaikin, P. *Phys. Rev. Lett.* **1993**, *70*, 3091.
(151) Bouffard, S.; Ribault, M.; Brusetti, R.; Jérome, D.; Bechgaard, K. *J. Phys. C* **1982**, *15*, 295.
(152) Choi, M.; Chaikin, P.; Huang, S.; Haen, P.; Engler, E.; Greene, R. *Phys. Rev. B* **1982**, *25*, 6208.
(153) Abrikosov, A. *J. Low Temp. Phys.* **1983**, *53*, 359.
(154) Zuppirolli, L. In *Low Dimensional Conductors and Superconductors*; Jérome, D., Caron, L. G., Eds.; Plenum Press: New York, 1987.
(155) Sanquer, M.; Bouffard, S. *Mol. Cryst. Liq. Cryst.* **1985**, *119*, 147.
(156) Johannsen, I.; Bechgaard, K.; Jacobsen, C. S.; Rindorf, G.; Thorup, N.; Mortensen, K.; Mailly, D. *Mol. Cryst. Liq. Cryst.* **1985**, *119*, 277.
(157) Mortensen, K.; Engler, E. M. *Phys. Rev. B* **1984**, *29*, 842.
(158) Tomić, S.; Jérome, D.; Mailly, D.; Ribault, M.; Bechgaard, K. *J. Phys.* **1983**, *44, C3*, 1075.
(159) Ravy, S.; Moret, R.; Pouget, J. P.; Comès, R. *Physica* **1986**, *143B*, 542.
(160) Maki, K.; Won, H.; Haas, S. *Phys. Rev. B* **2004**, *69*, 012502.
(161) Larkin, A. I. *JETP Lett.* **1965**, *2*, 130.
(162) Lebed, A. *JETP. Lett.* **1986**, *44*.
(163) Dupuis, N.; Montambaux, G.; de Melo, C. A. R. S. *Phys. Rev. Lett.* **1993**, *70*, 2613.
(164) Lee, I. J.; Brown, S.; Clark, W. G.; Strouse, M. J.; Naughton, M. J.; Kang, W.; Chaikin, P. M. *Phys. Rev. Lett.* **2002**, *88*, 017004.
(165) Jérome, D.; Pasquier, C. R. In *Superconductors*; Narlikar, A. V., Ed.; Springer-Verlag: Berlin, 2005.
(166) Mayaffre, H.; Wzietek, P.; Lenoir, C.; Jérome, D.; Batail, P. *Phys. Rev. Lett.* **1995**, 75.
(167) Kanoda, K.; Miyagawa, K.; Kawamoto, A.; Nakazawa, Y. *Phys. Rev. B* **1996**, 54.
(168) Kamiya, S.; Shimojo, Y.; Tanatar, M.; Ishiguro, T.; Yamochi, H.; Saito, G. *Phys. Rev. B* **2002**, 65.
(169) Zuo, F.; Brooks, J.; McKenzie, R.; Schlueter, J. A.; Williams, J. *Phys. Rev. B* **2000**, 61.
(170) Vuletić, T.; Auban-Senzier, P.; Pasquier, C.; Tomić, S.; Jérome, D.; Héritier, M.; Bechgaard, K. *Eur. Phys. J. B* **2002**, *25*, 319.
(171) Lee, I.; Naughton, M.; Chaikin, P. *Phys. Rev. Lett.* **2002**, *88*, 207002.
(172) Greene, R.; Engler, E. *Phys. Rev. Lett.* **1980**, *45*, 1587.
(173) Brusetti, R.; Ribault, M.; Jérome, D.; Bechgaard, K. *J. Phys. IV* **1982**, *43*, 801.
(174) Wilhelm, H. Unpublished data, 2004.
(175) Giamarchi, T. *Quantum Physics in One-Dimension*; Clarendon Press: Oxford, U.K., 2004.
(176) Schulz, H. J. *Phys. Rev. Lett.* **1990**, *64*, 2831.
(177) Voit, J. *Rep. Prog. Phys.* **1995**, *58*, 977.
(178) Solyom, J. *Adv. Phys.* **1979**, *28*, 201.
(179) Giamarchi, T. *Physica* **1997**, *B230−232*, 975.
(180) Jacobsen, C. S.; Tanner, D.; Bechgaard, K. *Phys. Rev. Lett.* **1981**, *46*, 1142.
(181) Jacobsen, C.; Tanner, D.; Bechgaard, K. *Phys. Rev. B* **1983**, *28*, 7019.
(182) Jacobsen, C. In *Low Dimensional Conductors and Superconductors*; Jérome, D., Caron, L. G., Eds.; Plenum Press: New York, 1987; p 253.
(183) Vescoli, V.; Degiorgi, L.; Henderson, W.; Grüner, G.; Starkey, K. P.; Montgomery, L. *Science* **1998**, *281*, 1181.
(184) Moser, J.; Gabay, M.; Auban-Senzier, P.; Jérome, D.; Bechgaard, K.; Fabre, J. M. *Eur. Phys. J. B* **1998**, *1*, 39.
(185) Mott, N. *Metal−Insulator Transitions*; Taylor and Francis: London, 1974.
(186) Moser, J.; Cooper, J. R.; Jérome, D.; Alavi, B.; Brown, S.; Bechgaard, K. *Phys. Rev. Lett.* **2000**, 84.
(187) Mihaly, G.; Kezsmarki, I.; Zamborsky, F.; Forro, L. *Phys. Rev. Lett.* **2000**, 84.
(188) Korin-Hamzić, B.; Tafra, E.; Basletić, M.; Hamzic, A.; Unterreiner, G.; Dressel, M. *Phys. Rev. B* **2003**, 67.
(189) Auban, P. To be published.
(190) Yakovenko, V.; Zhelenyak, A. T. *Synth. Met.* **1999**, *103*, 2202.
(191) Lopatin, A.; Georges, A.; Giamarchi, T. *Phys. Rev. B* **2001**, 63.
(192) Anderson, P. *The Theory of Superconductivity in the High T_c Cuprates*; Princeton University Press: 1997.
(193) Valla, T.; Johnson, P.; Yusof, Z.; Wells, B.; Li, W.; Loureiro, S.; Cava, R.; Mikami, M.; Mori, Y.; Yoshimura, M.; Sasaki, T. *Nature* **2002**, *417*, 627.
(194) Hussey, N.; Brien, M. M.; Balicas, L.; Brooks, J.; Horii, S.; Ikuta, H. *Phys. Rev. Lett.* **2002**, *89*, 086601.
(195) Brazovskii, S.; Gordyunin, S. *JETP Lett.* **1980**, *31*, 371.
(196) Auban, P.; Jérome, D.; Carcel, C.; Fabre, J. *J. Phys. IV* **2004**, *114*, 41; and to be published.
(197) Bourbonnais, C. In *High Magnetic Field*; Berthier, C., Levy, L. P., Martinez, G., Eds.; Springer: Berlin, 2002; p 236.
(198) Auban-Senzier, P.; Jérome, D.; Moser, J. In *Physical Phenomena at High Magnetic Fields*; Fisk, Z., Gorkov, L., Schrieffer, R., Eds.; World Scientific: Singapore, 1999 (http://www.worldscibooks.com/physics/3945.html).
(199) Schwartz, A.; Dressel, M.; Grüner, G.; Vescoli, V.; Degiorgi, L.; Giamarchi, T. *Phys. Rev. B* **1998**, *58*, 1261.
(200) Barisić, S.; Brazovskii, S. In *Recent Developments in Condensed Matter Physics*; Devreese, J. T., Ed.; Plenum Press: New York, 1981; Vol. 1, p 327.
(201) Emery, V. J.; Bruinsma, R.; Barisić, S. *Phys. Rev. Lett.* **1982**, *48*, 1039.
(202) Georges, A.; Giamarchi, T.; Sandler, N. *Phys. Rev. B* **2000**, *61*, 16393.
(203) Timusk, T. In *Low Dimensional Conductors and Superconductors*; Jérome, D., Caron, L. G., Eds.; Plenum Press: New York, 1987; p 275.
(204) Kikuchi, K.; Ikemoto, I.; Yakushi, K.; Kuroda, H.; Kobayashi, K. *Solid State Commun.* **1982**, *42*, 433.
(205) Ng, H.; Timusk, T.; Jérome, D.; Bechgaard, K. *Phys. Rev. B* **1985**, *32*, 8041.
(206) Ng, H.; Timusk, T.; Bechgaard, K. *J. Phys.* **1983**, *44*, C3-867.
(207) Heuzé, K.; Fourmigué, M.; Batail, P.; Coulon, C.; Clérac, R.; Canadell, E.; Auban-Senzier, P.; Ravy, R.; Jérome, D. *Adv. Mater.* **2003**, 15.
(208) Cooper, J. R.; Forró, L.; Korin-Hamzić, B.; Bechgaard, K.; Moradpour, A. *Phys. Rev. B* **1986**, 33A.
(209) Chaikin, P. *J. Phys. I* **1996**, *6*, 1875.
(210) Williams, J. *Organic Superconductors (including Fullerenes)*; Prentice Hall: Upper Saddle River, NJ, 1992.
(211) Graja, A. *Low Dimensional Organic Conductors*; World Scientific: Singapore, 1992.
(212) *Common Trends in Synthetic Metals and High Tc Superconductors*; J. Physique I, Vol. 6; EDP Sciences: Les Ulis, France, 1996; I. F. Schegolev memorial volume.
(213) Bernier, P., Lefrant, S., Eds. *Advances in Synthetic Metals, Twenty Years of Progress in Science and Technology*; Elsevier: New York, 1999.
(214) *Organic Superconductivity 20th Anniversary*; J. Physique IV France, Vol. 10 Pr3; EDP Sciences: Les Ulis, France, 2000.
(215) Jérome, D.; Schulz, H. *Adv. Phys.* **2002**, *51*, 293 (recent reprint of ref 25).
(216) *Symposium on Crystalline Organic Metals ISCOM2003*; J. Physique IV (France), Vol. 114; EDP Sciences: Les Ulis, France, 2004.
(217) Farges, J., Ed. *Organic Conductors*; Marcel Dekker: New York, 1994.